LA--710

Series B

UNCLASSIFIED

LA-710

Series B

28 October 1948   This document contains 80 pages.

NEUTRON FISSION CROSS SECTION OF U^{238} IN

THE REGION OF NEUTRON ENERGY BETWEEN 6 AND 9 MEV

Work done by:

B. R. Curtis
K. W. Erickson
J. L. Fowler
L. Rosen
J. Slye
P. H. Snowden
R. Squires
E. Stovall, Jr.
F. K. Tallmadge

Report written by:

B. R. Curtis
J. L. Fowler
L. Rosen

UNCLASSIFIED

UNCLASSIFIED

UNCLASSIFIED

UNCLASSIFIED

- 2 -

Abstract

Apparatus has been developed for using the
cyclotron to produce effectively monoenergetic neutrons.
The $D(d,n)He^3$ reaction is used, the bombarding deuterons
being accelerated to about 10 Mev by the Los Alamos
Cyclotron. The energy of these deuterons is determined
by deflection in a magnetic field. The He^3 particles
emitted into known solid angle and having known energy
are counted by a proportional counter. A fission counter
having foils on which is deposited uniform determined
weights of U^{238} is placed in the path of the neutrons
associated with the He^3 particles. Coincidences between
the He^3 counter and the fission counter are recorded.
The resolving time of the apparatus, and hence the ac-
cidental coincidences, are determined by moving the fis-
sion counter to such an angle that no real coincidences
can occur. Since the proportional counter records the
He^3 flux, and hence the associated neutron flux, the
cross section of "28" is determined from the real
coincidences per He^3 count and the thickness of the U^{238}
in the path of the neutrons. The values of the cross
section obtained together with the standard errors are:

$$\sigma \ (E_n = 8.8 \pm 0.5) = 1.17 \pm .11 \text{ barns}$$
$$\sigma \ (E_n = 5.6 \pm 0.5) = 0.68 \pm .14 \text{ barns}$$
$$\sigma \ (E_n = 8.9 \pm 0.5) = 1.04 \pm .12 \text{ barns}$$

UNCLASSIFIED

UNCLASSIFIED

NEUTRON FISSION CROSS SECTION OF U^{238} IN

THE REGION OF NEUTRON ENERGY BETWEEN 6 AND 9 MEV

Introduction

At Los Alamos it is necessary to know the neutron fission cross section of U^{238} from the threshold to the region of 14 Mev (LA-610).

A number of investigators have determined the cross section for neutron energies below 3 Mev (see LA-520). With the $D(d,n)He^3$ reaction on the "long" electro-static generator, the data has been extended to 5.85 Mev (LA-530). More recently, neutrons from the $T(d,n)He^4$ reaction have been used to obtain the cross section at 14 Mev and above (LAMS-777). There was, however, no standard way to produce monoenergetic neutrons in the region from 6 Mev to 14 Mev. In spite of the high neutron background associated with cyclotrons, a method has been developed to use the 10 Mev deuterons to produce effectively monoenergetic neutrons of energies between 6 and 9 Mev. The $D(d,n)He^3$ reaction is used where only fissions in coincidence with He^3 particles are counted. (The cross section for this reaction at 10 Mev is sufficient for this problem). (LAMS-600, Phys. Rev. 73 648, (E-8)(648)).

UNCLASSIFIED

- 4 -

LA 710

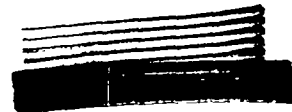## I. APPARATUS ASSEMBLY

In order to avoid the background in the immediate vicinity of the cyclotron, the deuteron beam was used 15 ft. from the cyclotron beyond the water wall shields. Fig. 1 shows the layout of apparatus. The deflected beam from the cyclotron is brought through 6" brass tubing to a wedge-shaped focusing magnet. From here the beam, being diaphragmed to $\pm$ 0.63°, passes through a gas target in the center of a 2 ft. diameter reaction chamber. Deuterium gas is contained in the target by mica windows over the entrance and exit ports and over a side tube for He^3 particles. These particles emitted into known solid angle, and hence having known energies, are counted by the proportional counter. The fission counter is rotated in a horizontal plane until it is centered on the cone of neutrons associated with the He^3 particles. The deuteron beam is monitored by a Faraday cup and recorded by an electronic current integrator.

From time to time the energy of the beam is determined by lifting the Faraday cup out of the path of the beam and allowing the beam to pass through slits and then between the poles of the analyzing magnet. A simultaneous measurement of the deflection of the beam and the magnetic field gives the deuteron energy.

UNCLASSIFIED

FOCUSING MAGNET

CYCLOTRON

DEFLECTOR

FISSION COUNTER

TRACK

BEAM DIRECTION

FARADAY CAGE SECTION

SLIT SECTION

REACTION CHAMBER

GAS TARGET

ANALYZING MAGNET

FLUORESCENT SCREEN

OIL DIFFUSION PUMP

OIL DIFFUSION PUMP

PROPORTIONAL COUNTER

SCALE IN INCHES

VACUUM SYSTEM
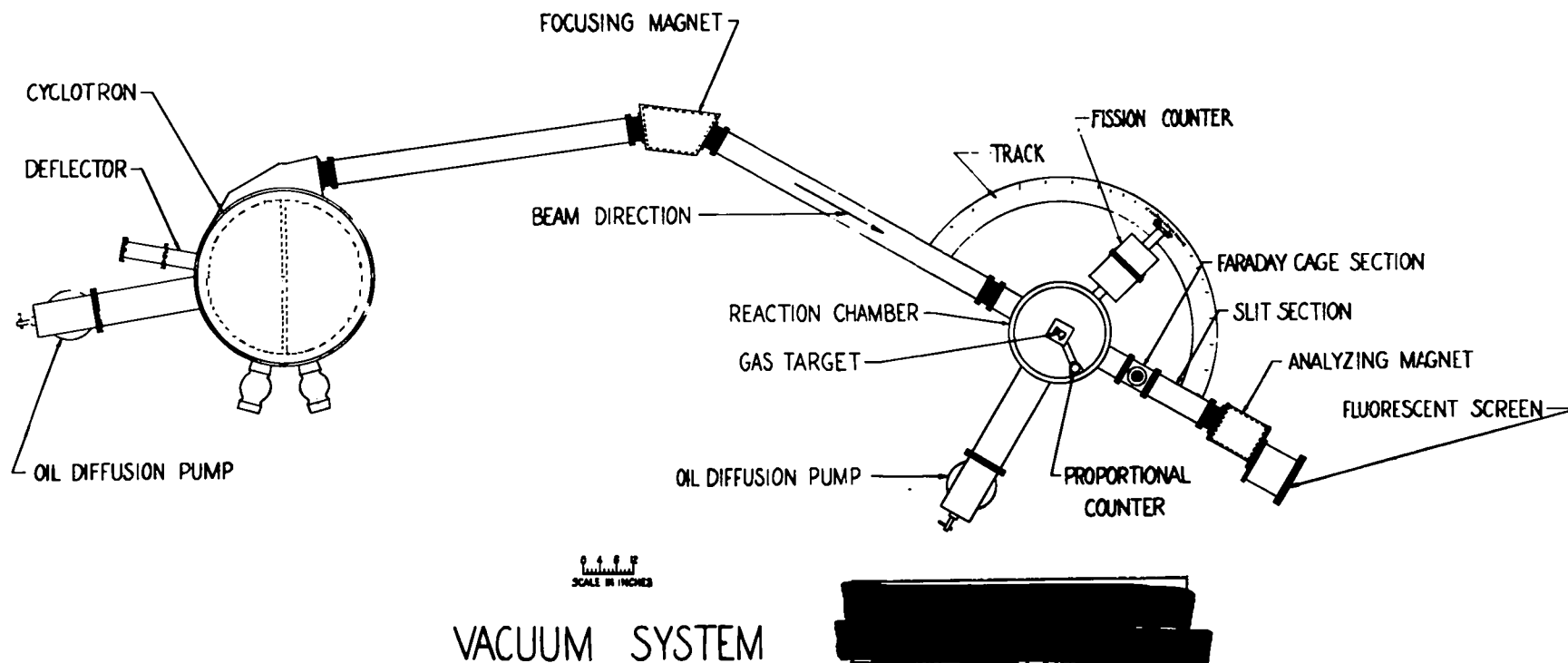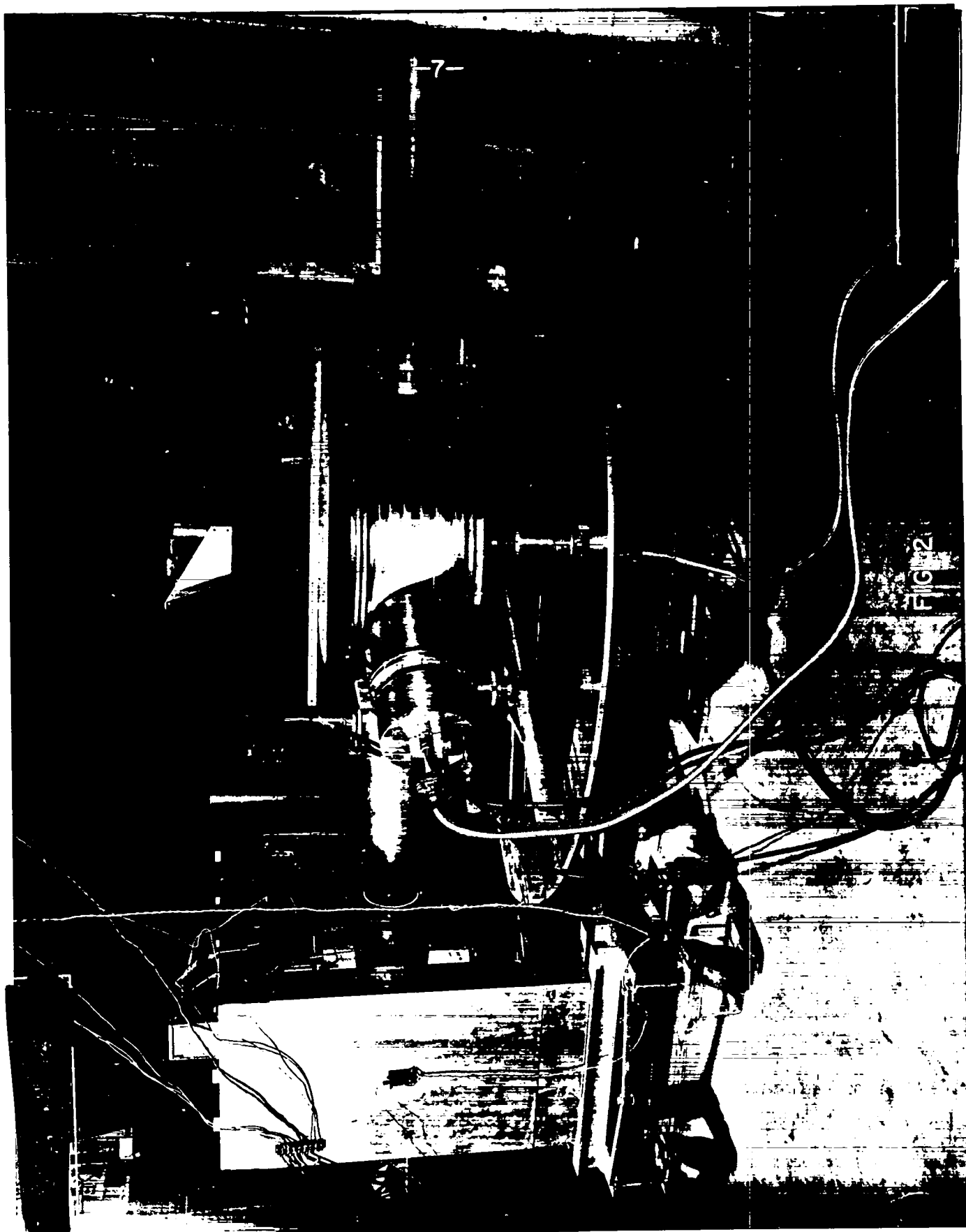
FIG 1

During a run the number of He^3 particles, the number of fissions, and the number of coincidences between them are recorded electronically. The number of accidental coincidences is found from the resolving time of the apparatus (approximately 2 μs) which is determined experimentally by runs in which the fission counter is rotated at such an angle that there can be no real coincidences.

Figs. 2 and 3 are photographs of the scattering chamber, fission counter, and analyzing magnet.

Figs. 4 and 5 are top and side view assembly drawings of the reaction chamber, proportional counter, and fission counter. The reaction chamber proper, pump out leads, and side ports are of welded steel construction. The lid of the reaction chamber is a 1-1/2" thick safety plate glass which rests on two 1/4" x 1/4" thick rubber gaskets which are countersunk in grooves in the ring around the edge of the chamber. The bottom of this chamber is a 3/4" brass plate which contains a 1/4" gasket groove to make the vacuum seal to the chamber. In the center of the bottom plate is a 2" diameter Wilson seal through which the proportional counter can be rotated at the desired angle to the beam in the horizontal plane. The lead to the proportional counter passes through the center of its supporting arm. The proportional

FIG. 2

FIG 3

GAS TARGET

FISSION COUNTER

8" GATE VALVE

BEAM

-9-

TO FARADAY CAGE &
ANALYSER MAGNET

D-D REACTION CHAMBER

FIG 4

GATE VALVE

1·1/2" THICK SAFETY GLASS

GAS TARGET

PROPORTIONAL COUNTER

FISSION COUNTER

8' OIL DIFFUSION PUMP
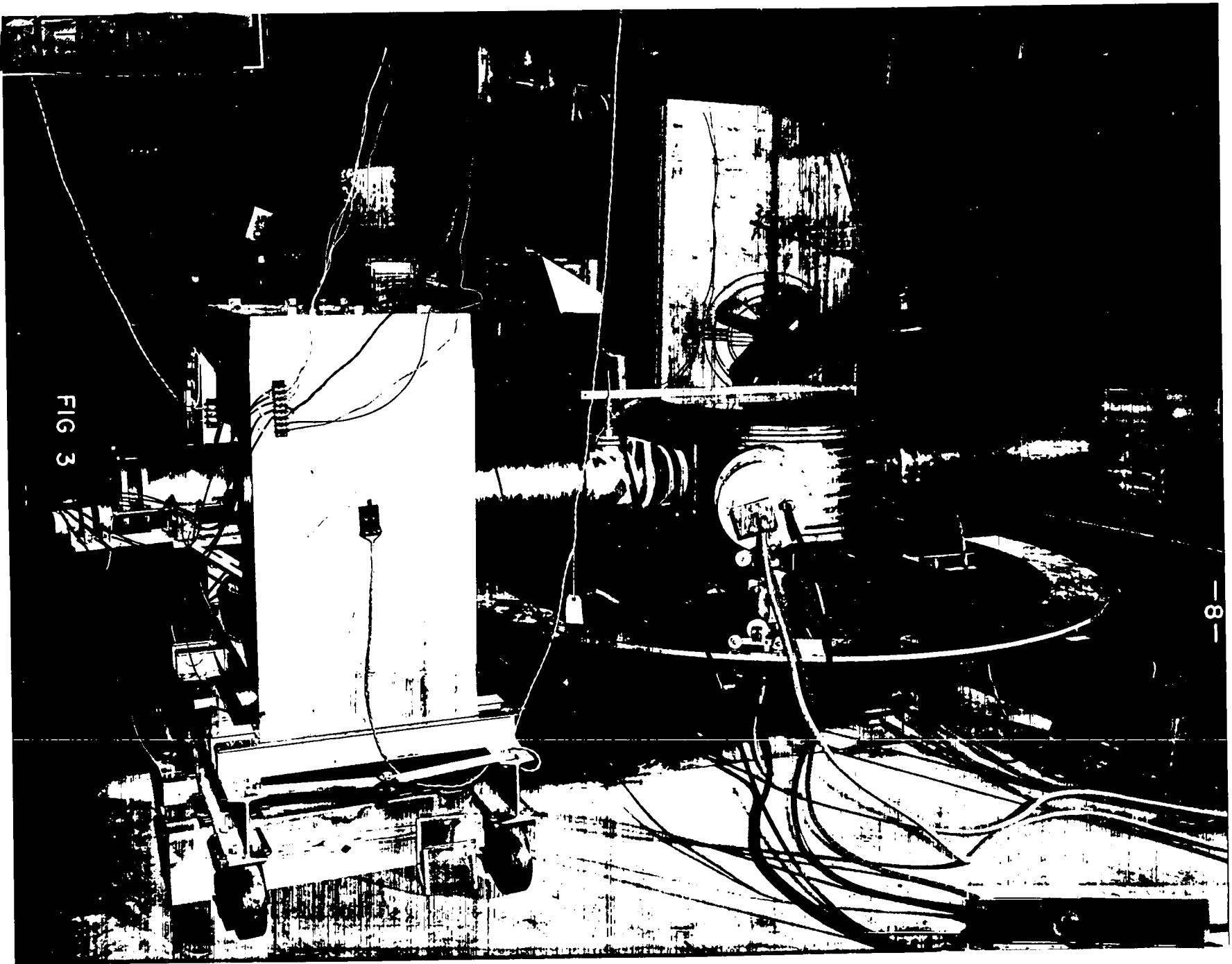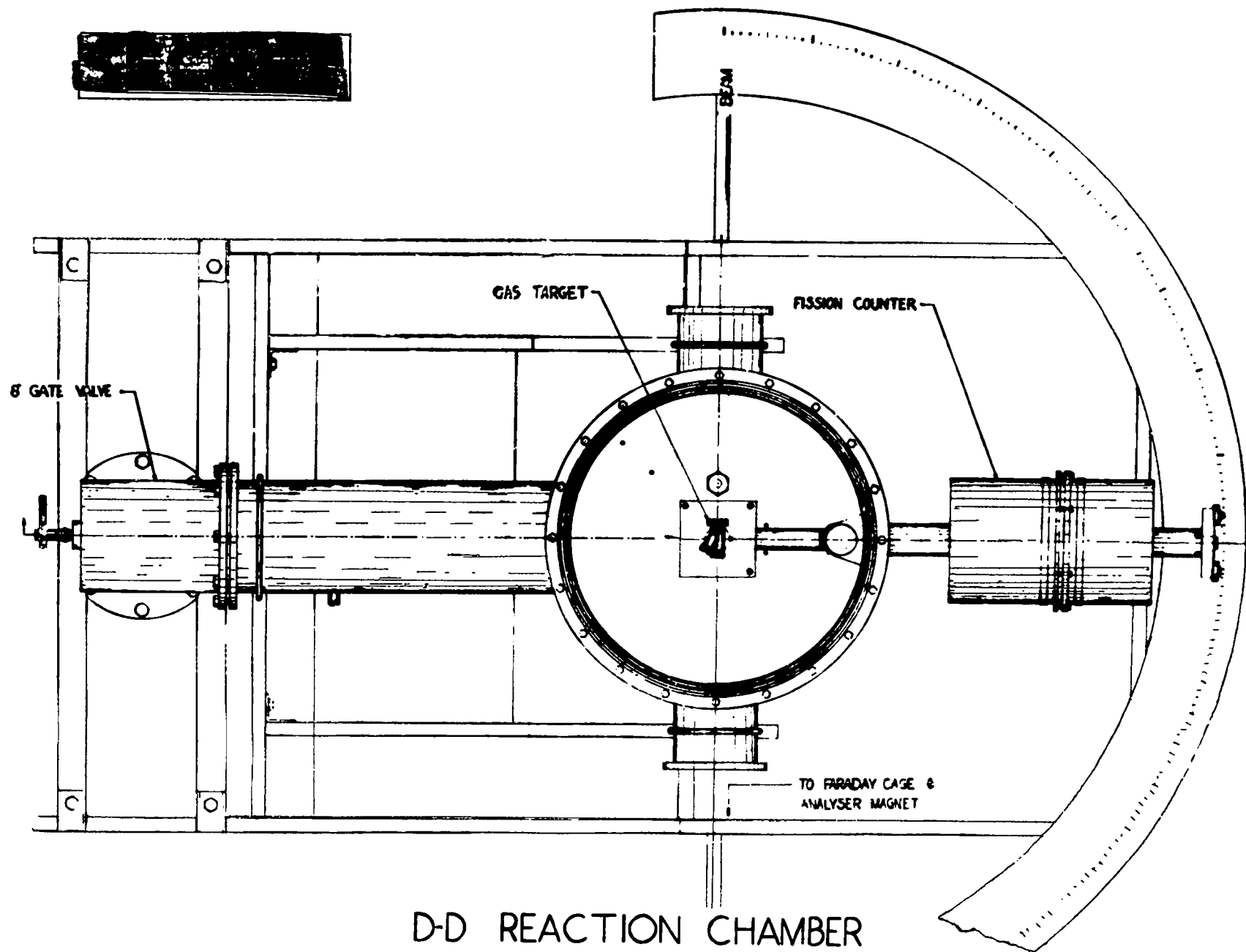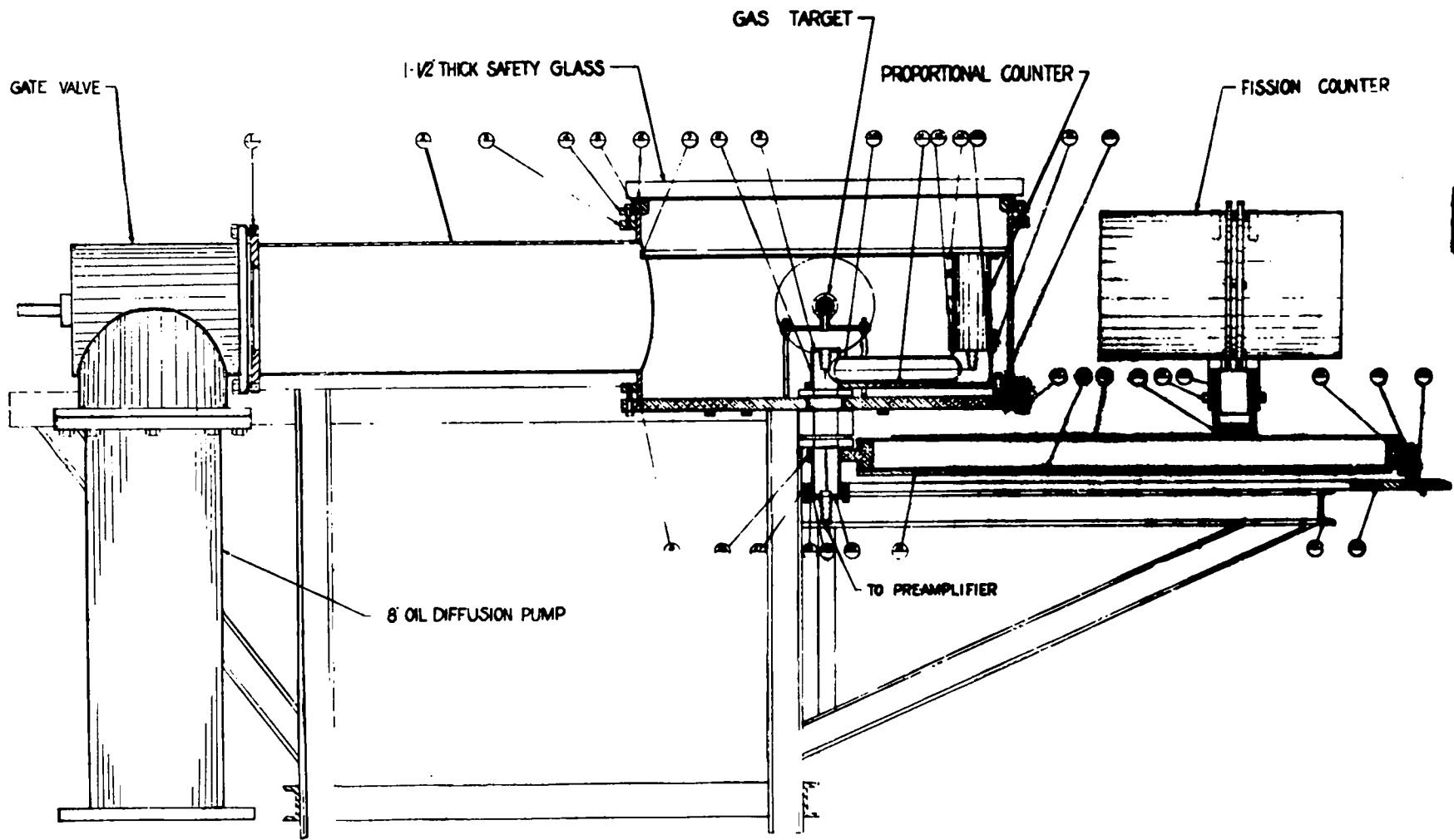
TO PREAMPLIFIER

D-D REACTION CHAMBER

FIG 5

counter is so mounted that it can be adjusted in height
relative to the base plate. The high voltage connections
and preamplifiers which can be seen in the photograph of
Fig. 2 are supported at the end of the 2" tube which
passes through the Wilson seal. Mounted within the re-
action chamber at about the top of the proportional counter
is a ring accurately graduated in degrees from 0 - 360°.
All angular measurements are referred to this ring. As
can be seen in the drawing of Fig. 4, the fission
counter is mounted on an arm outside of the reaction
chamber and can be rotated at any angle from 0 - 180°
about the center. The angular position of this counter
can be read on graduations on a semi-circular track
seen in Fig. 5, which is calibrated against the ring
within the reaction chamber. The height and radial
position of the fission counter are adjustable.

Fig. 21 is a drawing of a typical gas target,
which is supported on a mount above the base plate such
that it can be lined up with the geometrical center of
the reaction chamber. The windows over the ports are
mica of thickness from 1-3 mg/cm^2 depending on the an-
gular region being investigated. The target is so con-
structed that the proportional counter can only see
the beam where it is bombarding the target gas, and
hence the charged particle background due to bombardment

- 12 -

of windows, etc., is eliminated. Similar targets were used in which the side ports make angles of 20° and 30° with the beam axis.

Fig. 6 is a drawing of the Faraday cage section, showing how the Faraday cage can be removed from the path of the beam by means of the Wilson seal. Permanent bar magnets arranged to give a field at the bottom of the cup perpendicular to the axis of the beam immobilize secondary electrons produced by the beam.
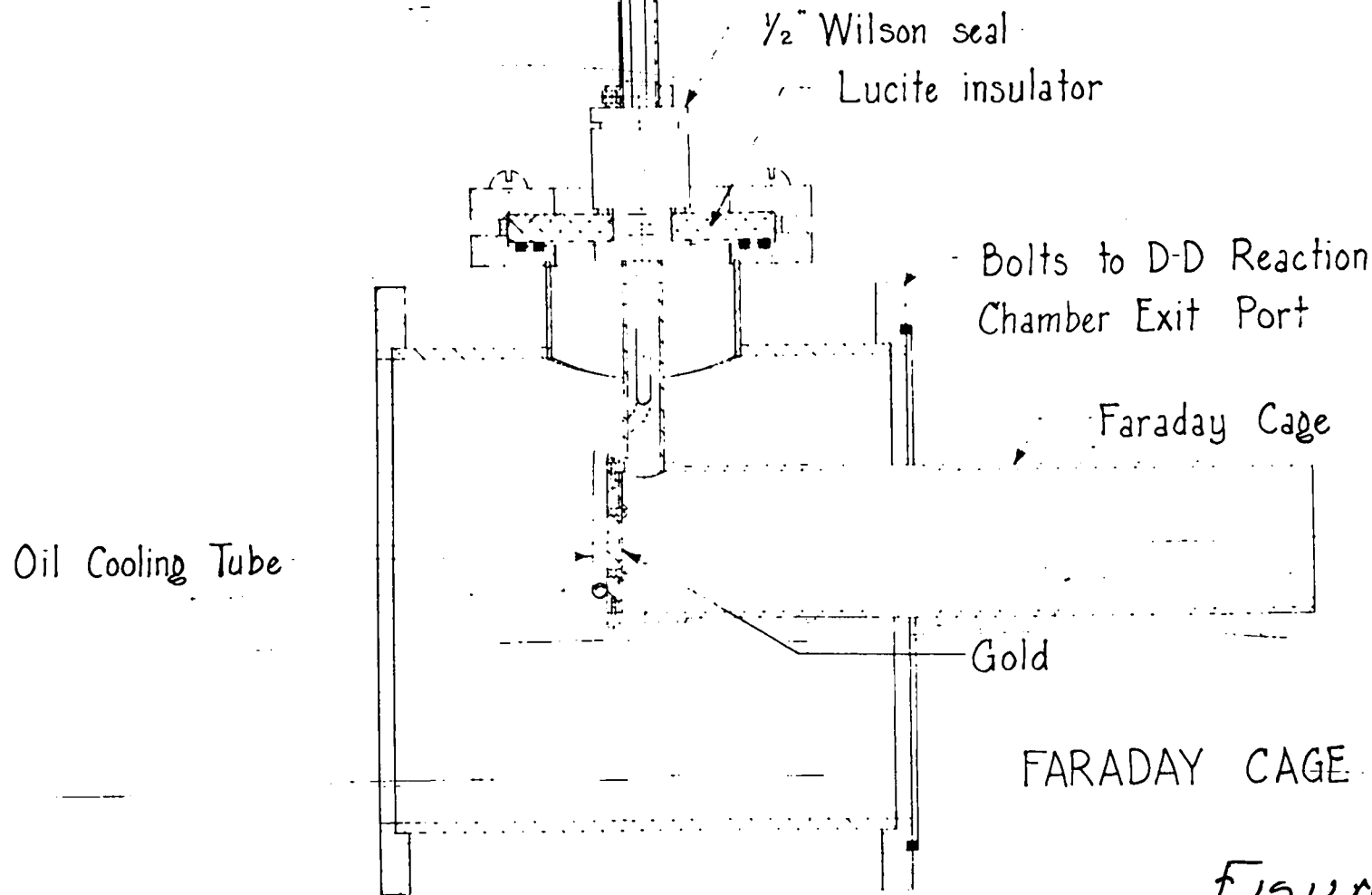
½" Wilson seal

Lucite insulator

Bolts to D-D Reaction Chamber Exit Port

Faraday Cage

Oil Cooling Tube

$1\frac{3}{4}$

Gold

FARADAY CAGE SECTION

Figure 6

- 14 -

LA 710

II. FOCUSING THE CYCLOTRON BEAM

In many experiments associated with a cyclotron
it is desirable to have the beam some distance from the
accelerating chamber, both for the reduction of neutron
background and for the ease of installation of experi-
mental apparatus. This was accomplished during the war
by Feynman, Lavatelli, and Sutton (LAMS-514) who used a
wedge-shaped magnet to focus a fairly intense beam of
deuterons outside of the cyclotron water shield about
fifteen feet from the cyclotron.

The general method outlined in the above report
was followed. Considerable time was spent adjusting the
position of the focus magnet and the target chamber
so that the best possible focus was obtained. These
adjustments were greatly facilitated by the use of a
television pickup and camera which permitted continuous
observation of the focused spot of deuterons, as observed
on a willemite (zinc orthosilicate) screen placed at
the end of the exit tube. By this means the best focal
distance was determined and also the best position of
the focus magnet with reference to the target. The
outline of the essential apparatus is shown in Fig. 7.
The willemite screen was placed on a glass plate at the
end of a telescoping tube which could then be adjusted
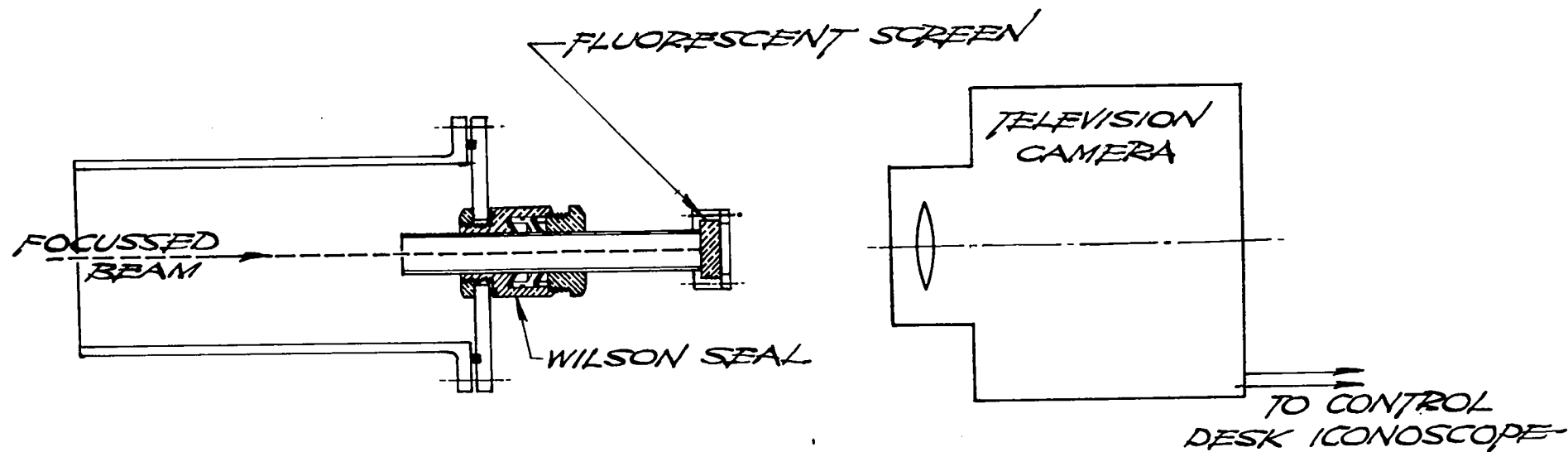to any desired distance and the effect on the focus

FLUORESCENT SCREEN

FOCUSSED
BEAM

TELEVISION
CAMERA

WILSON SEAL

TO CONTROL
DESK ICONOSCOPE

FIG. 7

EQUIPMENT FOR ADJUSTING FOCUS CONDITIONS

observed. The focused spot was approximately 1/4-inch
wide by 3/4-inch high and under the optimum operating
condition a beam of 5 microamperes of 10 Mev deuterons
could be obtained over this area.

One additional piece of equipment was added,
namely an electronic control (designed by H. T. Gittings -
LAMS-678) for the focusing magnet field so that it
could be maintained constant throughout any given ex-
periment.

Since the gas target is located approximately
at the focus point of the wedge-shaped magnet (300 cm
from the focusing wedge) the beam converges as it enters
the target and diverges as it leaves the center of the
scattering chamber. In order to restrain the beam to
a known direction a slit 1-1/8" wide by 13/16" high was
placed between the focus magnet and the scattering chamber
at a distance of 71.6" from the target and a gold
diaphragm with a 1/2" hole placed at the target entry port
so that the beam was defined to $\pm$ 0.63 degrees in the
horizontal and $\pm$ 0.53 degrees in the vertical direction.

To determine the exact direction of the beam
as it passes through the gas target chamber, a small
aperture (1/8" diameter) Faraday cup was mounted on the
proportional counter. This was moved through the beam
and the current picked up by the cup measured by a

DC amplifier. Thus the angular spread of the beam could be measured and its angular direction in passing through the scattering chamber determined. A sample curve of the angular spread is shown in Fig. 8. This is the spread expected from the geometry of the experiment. Rutherford scattering due to the front window of the gas target does not increase appreciably the angular spread, since only about 0.4% of the beam would be scattered more than one degree.

Under normal operating conditi ns one obtains a beam of deuterons on the exit port from the cyclotron which is sensitive to deflector voltage. With a high deflecting voltage the beam hitting the outside of the focus magnet may be 25 microamperes; by lowering the deflector voltage a beam of approximately 10 microamperes hits the inside of the exit tube. For optimum conditions one adjusts for the valley between the two peaks, which indicates that the maximum is hitting the 5" x 1/2" opening through the focus magnet. Conditions can also be varied so that very little current is striking the exit tube, which is desirable for the reduction of background.

The position of the deflector tilt is quite important to obtain a maximum beam at the target. In general, a tilt toward the Dee reduces the deflector

LA 710

LA 710
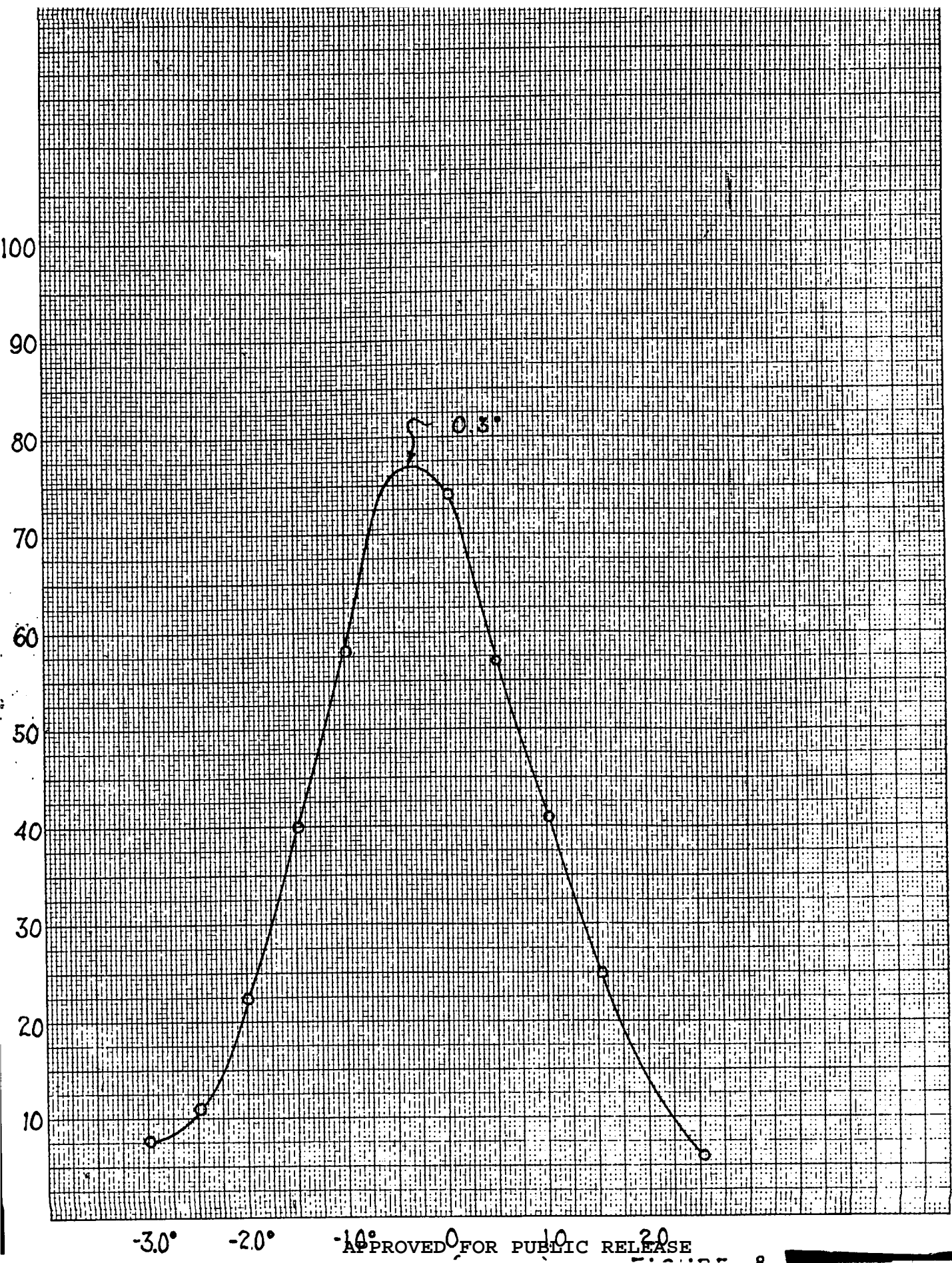
voltage necessary to hit the focus magnet; a tilt away
increases the voltage required.

The beam current was measured by means of a
Faraday cage (Fig. 1) connected to an electronic current
integrator (DWG. #704). The cage could be lifted through
a Wilson seal, so that the beam could pass through the
slit section and into the analyzing magnet, when the
energy of the beam was measured.

III. ENERGY MEASUREMENT

The energy of the beam of deuteron ions was measured by a magnetic deflection method following the general procedure described by Creutz and Wilson (RSI 17, 385, 1946). This involves the measurement of the deflection of the deuteron beam and the simultaneous measurement of the magnetic field causing the deflection.

A. Experimental Arrangement:

The experimental arrangement is shown in Fig. 9. It consists of a magnet with rectangular pole pieces (28.54 x 25 cm), a fluorescent screen for observation of the deuterons, and a single turn rectangular flux coil for measurement of the field. An adjustable slit section is provided between the gas target and the analyzing magnet to define the beam.

The energy of the deuteron beam is given approximately by the following formula, which is derived from the equations of motion (see Appendix I):

$$W = \frac{e^2 A^2}{2M_0 c^2} \left(1 - \frac{W}{2M_0 c^2}\right) x \left[1 + \left\{\frac{a + b/2(1 - e^2 A^2/8M_0 e^2 W)}{D}\right\}^2\right] \quad (1)$$

where W is the energy of the deuteron beam in ergs, D is the deflection as measured on the fluorescent screen, e is the charge on the deuteron, M_0 the rest mass of the deuteron, a and b are dimensions of the apparatus as shown in Fig. 9.
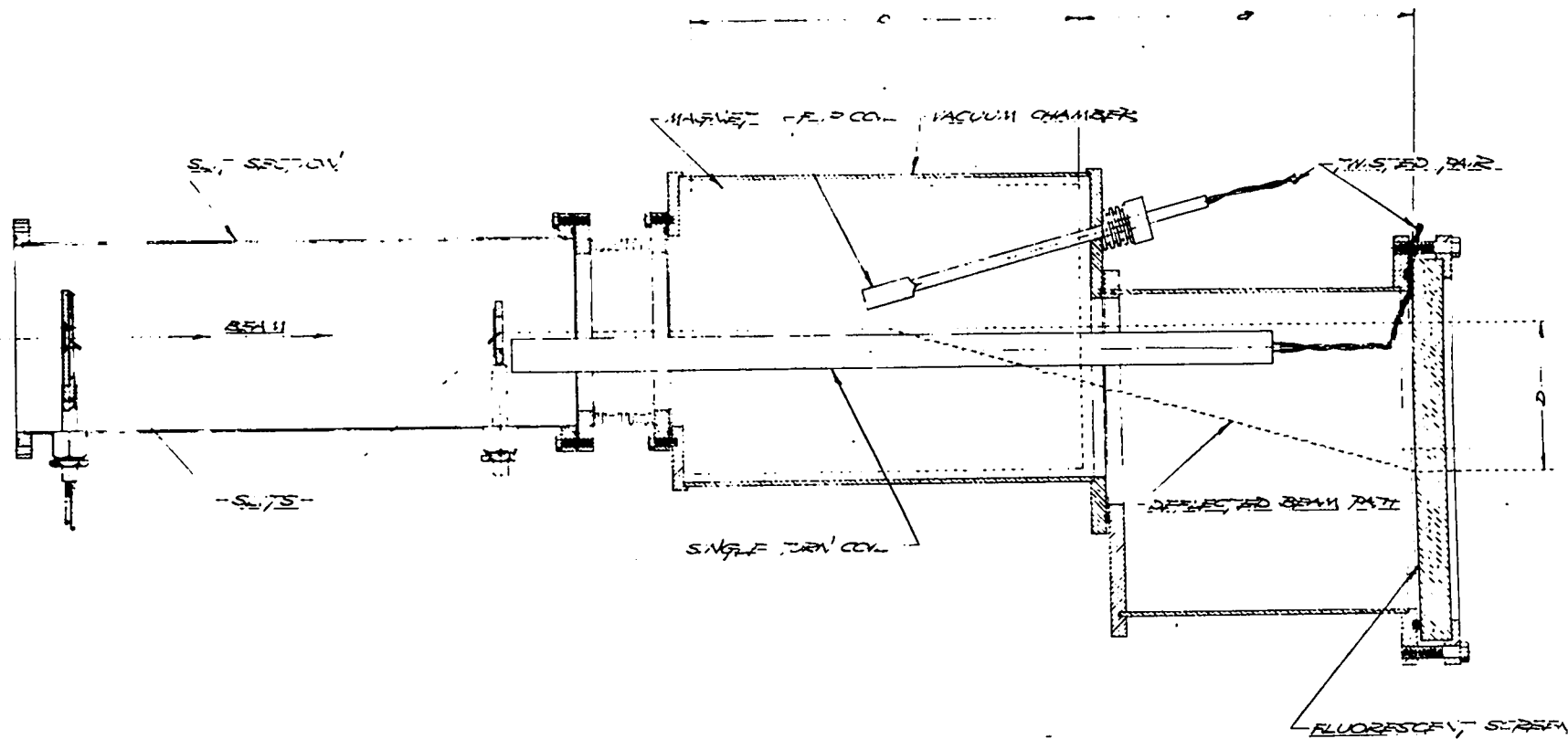
SLIT SECTION

MAGNET FIELD COIL   VACUUM CHAMBER

TWISTED PAIR

BEAM

SLITS

SINGLE TURN COIL

DEFLECTED BEAM PATH

FLUORESCENT SCREEN

FIGURE 9

ENERGY MEASURING SECTION

- 22 -

B. Measurement of Field:

The quantity A in Equation (1) is equal to $\int Hdx$ where H is the change in magnetic field produced by breaking the magnetizing current and x is measured along the initial direction of the deuteron beam. The value of A is determined by use of the single turn coil of width W which extends through the magnetic field from a zero field region on one side of the magnet to a zero field region on the other. The ends of this coil are brought out with a twisted pair to reduce the effect of stray fields and connected to the secondary of a mutual inductance M as shown in Fig. 10. The coil was constructed by winding a single turn of 0.001 inch copper strap around a rectangular lucite form. The form was accurately machined so that the width, W, of the completed coil was 1.033 $\pm$ 0.002 inches. The total flux as measured with the coil is equal to $w \int Hdx$ which is equal to $M \Delta I$ where ΔI is the current through the primary of M necessary to balance out the emf developed by the change in flux through the coil. The current ΔI was measured with a potentiometer bridge and standard resistance.

Since in this method only a single deflection was measured rather than reversing the magnetic field, as was the case in the method of Creutz and Wilson,

SINGLE TURN
TEST COIL

LEEDS & NORTHRUP
GALVANOMETER #653555
SENSITIVITY = .0000095μa/mm.
PERIOD = 42 SEC.

POTENTIOMETER

3000 Ω SHUNT

M

MUTUAL INDUCTANCE

R 10 Ω STANDARD
RESISTANCE

FIG. 10

CIRCUIT FOR MEASURING MAGNETIC FIELD

- 24 -

a small correction was necessary for the residual field
of the magnet. This was obtained by using a small flip
coil, which was calibrated against the single turn coil
so that the residual field could be measured and the
correction applied. Since the residual field causes
compensating correction in both D and H the correction to
the energy is small. The advantage of measuring the field
by breaking the current to the magnet rather than rever-
sing this current lies in the fact that the time constant
in the former case is short enough to eliminate a cor-
rection for galvanometer drift.

C. Discussion of Errors:

The mutual inductance used in these experiments
is calibrated by Leeds and Northrup to $\pm$ 0.5% accu-
racy. It was compared with two other inductances and
found to agree within 0.2%.

The width of the undeflected deuteron beam
was approximately one mm wide. When deflected the width
increased about 0.5 mm, indicating a spread of energy
within the beam of approximately 1%. The position of
the beam could be read to 0.5 mm in 160 mm, or a maxi-
mum error of 0.3%.

The geometrical constants a, b, and w could be
measured to better than 0.2%.

Since the energy is proportional to A^2/D^2

- 25 -

the expected accuracy is of the order of $\pm$ 2%.

Since a null method is used for measurement of
the flux the error introduced by galvanometer drift
is negligible.

Examples of energy measurements for three runs
are given in Appendix II.

D. __Absorption Measurements__:

Several tests were made using aluminum ab-
sorbers to take out most of the energy of the deuteron
beam and then varying the gas pressure in the target
chamber to give a range-absorption curve for the beam.
The results of the method showed essential agreement
with the magnetic deflection method and indicated that
no large error existed, i.e., a shorted pick up coil,
etc..

- 26 -

IV. ELECTRONIC EQUIPMENT

Fig. 11 is a block diagram of the electronic equipment used. All of the equipment is of standard design and is identified by the following designations:

Pre-amplifiers and main amplifiers - Model 500

Coincidence Circuit   - Dwg. 808

Current Integrator   - Dwg. 704

Scalers   - Model 200

Mechanical Counter - Cyclotron Specialties Co.

10 Channel Amplitude Analyzer   - Model 301

Precision Pulser   - Model 100

The only change made in the electronic equipment consisted in replacing the R-C clippers in the main amplifiers with delay line clippers which reduced the pulses to about 1/5 of their original amplitudes in about 2 μs.

This was accomplished by terminating the last cathode follower in the pre-amplifier with a resistance to ground equivalent to the input resistance of the main amplifier, and inserting between the output of the pre-amplifier and the input of the main amplifier the circuit shown in Fig. 12.

Each channel of the coincidence circuit produced pulse gates 0.85 μs wide. The resolving time of the coincidence circuit was experimentally determined

BLOCK DIAGRAM OF ELECTRONIC EQUIPMENT

```
┌─────────────────┐              ┌─────────────────┐
│  PROPORTIONAL   │              │    FISSION      │
│    COUNTER      │              │    CHAMBER      │
└─────────────────┘              └─────────────────┘
         │                                │
┌─────────────────┐              ┌─────────────────┐
│  PRE-AMPLIFIER  │              │  PRE-AMPLIFIER  │
└─────────────────┘              └─────────────────┘
         │                                │
┌─────────────────┐              ┌─────────────────┐
│      MAIN       │              │      MAIN        │
│   AMPLIFIER     │              │   AMPLIFIER      │
└─────────────────┘              └─────────────────┘
```

COINCIDENCE CIRCUIT

SCALER

SCALER

MECHANICAL COUNTER

MECHANICAL COUNTER

10 CHANNEL AMPLITUDE ANALYZER
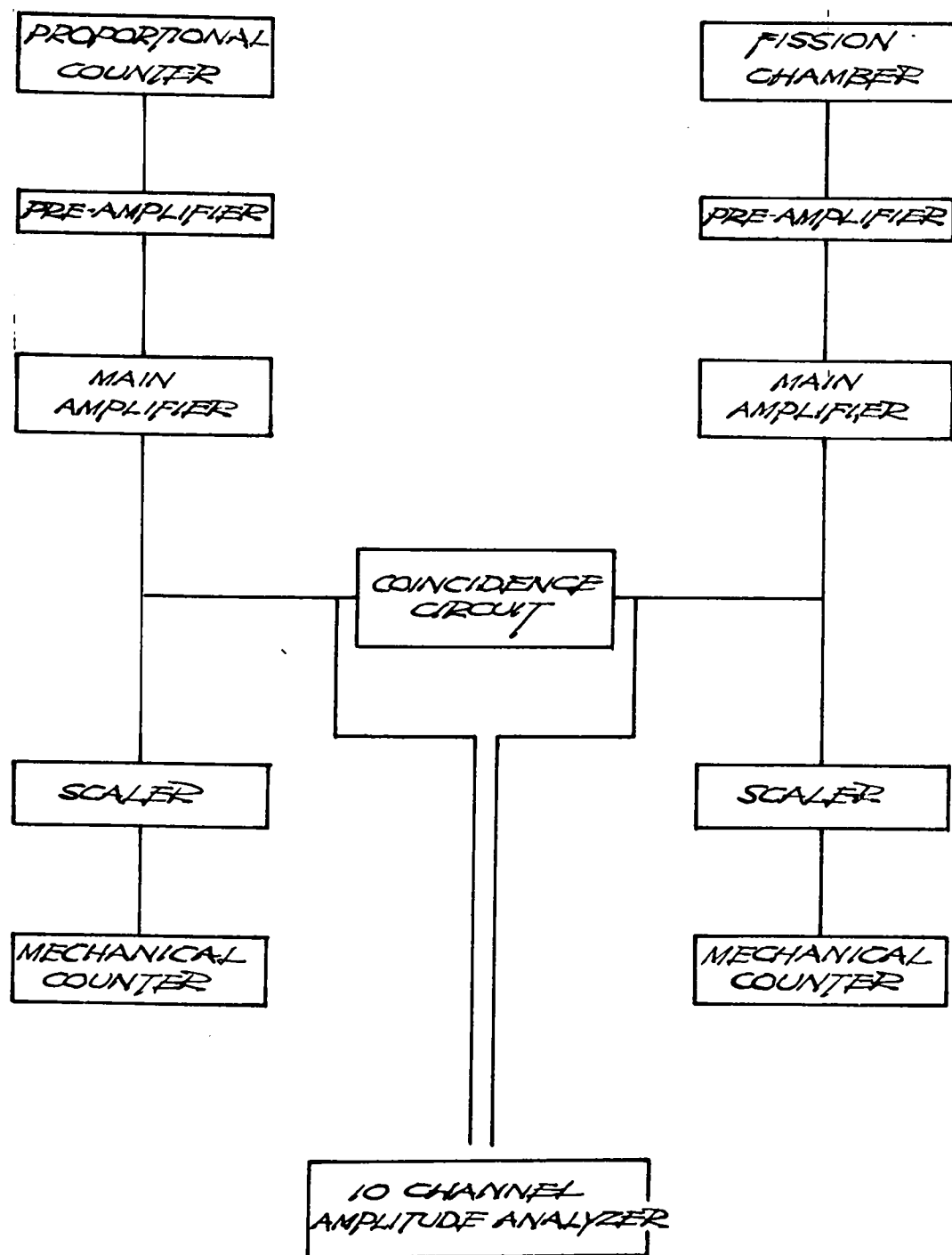
FIG. 11

DELAY LINE CLIPPER ARRANGEMENT USED
WITH AMPLIFIERS

OUTPUT TO PREAMP → ┤├ ⌇⌇⌇ → INPUT TO MAIN AMPLIFIER

0.1 μF.   500

0.5 μ S. SHORTED
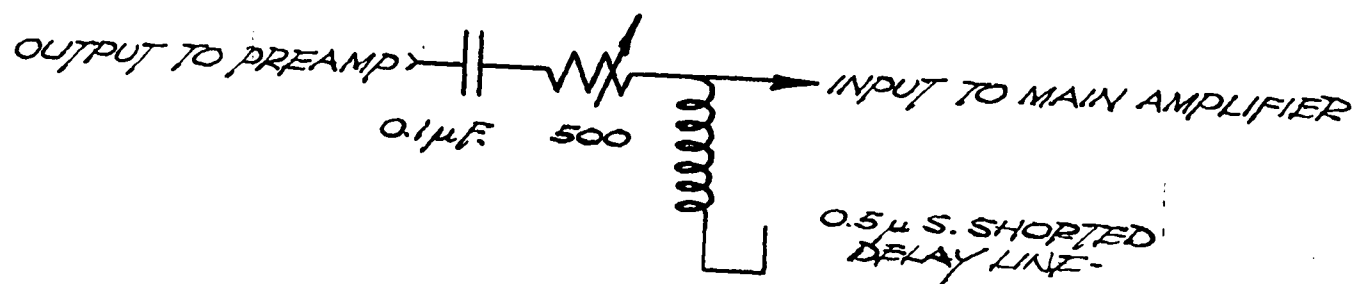DELAY LINE-

FIG. 12

- 29 -

with the same counters used in the actual experiment,
as described in Section VIII. - H. This experimental
resolving time came very close to the previously de-
termined electronic resolving time.

A precision pulser was used to intercalibrate
amplifiers, discriminators, and 10 channel amplitude
analyzer at the beginning and end of approximately
each four-hour period.

LA 710

V. FISSION COUNTER

Fig. 13 is a sectional assembly of the fission chamber used. It consisted of 13 plates, 7 of which served as collectors while the other 6 served as the high voltage electrodes and contained U^{238} foils on both sides. Each plate was made of 1/32" dural, the spacing between plates being 0.396". The counter was filled with argon to a pressure of 35#/sq. inch above atmosphere. This pressure was more than sufficient to stop the most energetic fission particles before they reached the collecting electrodes. The gas filling was renewed every 12 hours in order to avoid changes in pulse sizes due to accumulation of impurities in the gas. A voltage of 4000 volts, well filtered by a π network of resistors and capacitors, was applied to the high voltage electrodes. It was determined that changing the voltage by 1000 volts in either direction had no effect on the number of pulses recorded at the bias setting employed.

The fission pulses, as seen on an oscilloscope, had a rise time of slightly less than 1 μs and a width of about 2 μs. Random noise was considerably lower than the pulses produced by the α- particles from the active material. α pileup was negligible. The U^{238} foils for this experiment were made by R. W. Potter. The foils were made by the Zapon technique, the painting
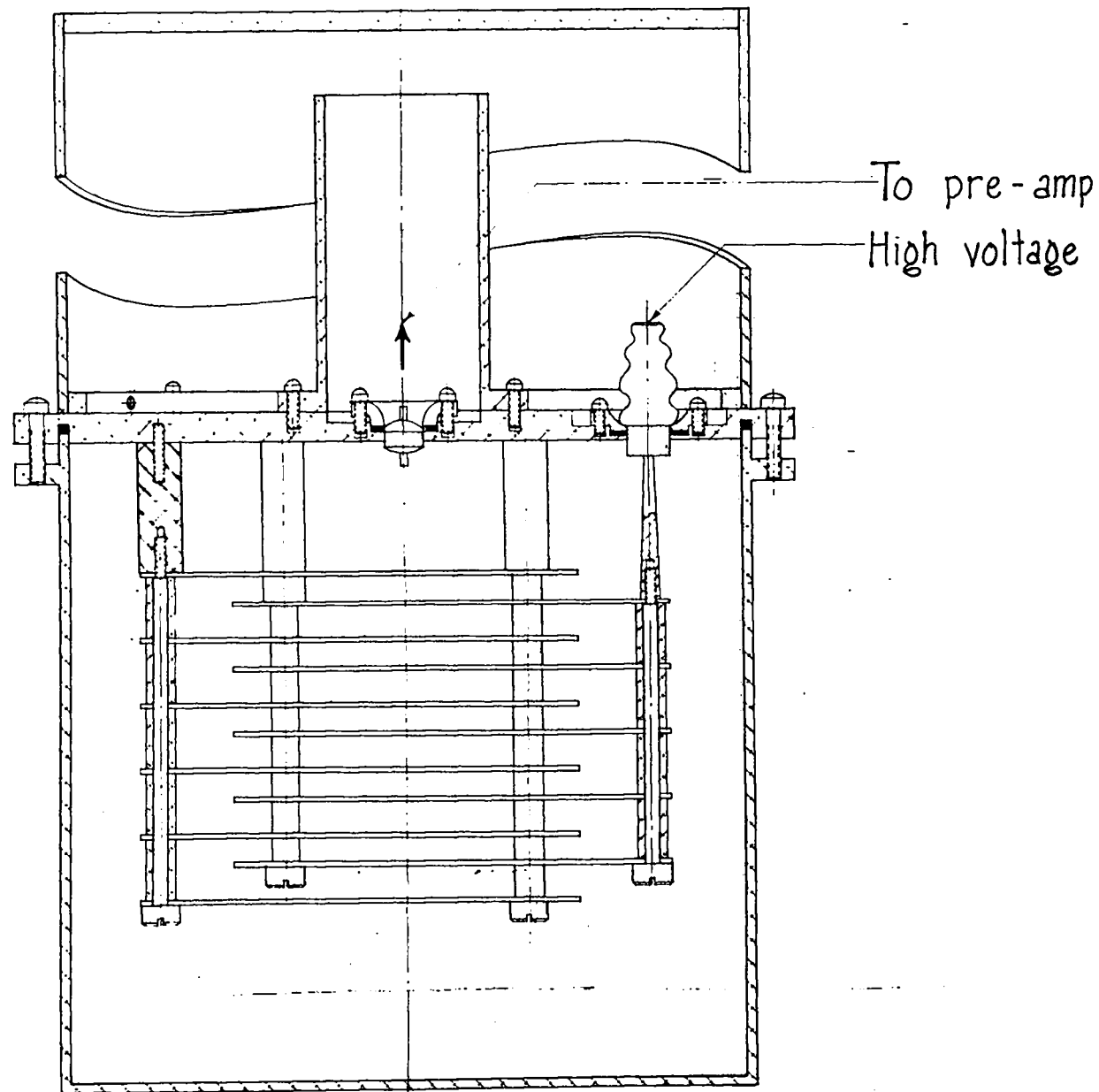
To pre-amp

High voltage

FIGURE 13
Fission Counter

- 32 -

being done mechanically on an endless belt moving
past a stationary brush into which was fed the Zapon
solution containing U^{238}. By this method it was possible
to obtain foils which were uniform in thickness to better
than 10%. The uniformity of the foils was determined
by placing each foil in contact with an α-particle
sensitive photographic emulsion for an appropriate
time. After exposure the plates were processed and
examined under a microscope and the number of α-parti-
cles/unit area was determined for 10 to 12 areas on each
foil. This determined the uniformity of the foils over
very small areas (~ 0.1 mm^2). Fig. 14 is a plot of
the number of tracks per unit area as a function of
distance from the center of a typical foil. Although
the non-uniformities did exhibit somewhat of a pattern,
most of this was eliminated by the ramdom mounting of the
foils in the counter. The foils were mounted on the
dural high voltage plates with liquid porcelain cement.
This eliminated most of the impurity difficulties which
are involved when one uses lucite or duco cement. Even
so, it was found desirable to expose the plates to a
fairly good vacuum ($\sim 10^{-4}$ mm Hg) for 24 hours after
the foils were mounted. Fig. 15 gives the energy dis-
tribution of the fission fragments as observed in the
fission counter under normal operating conditions.

Variation Of U²³⁸ Foil Thickness With Distance From Center Of Foil

FIGURE 14

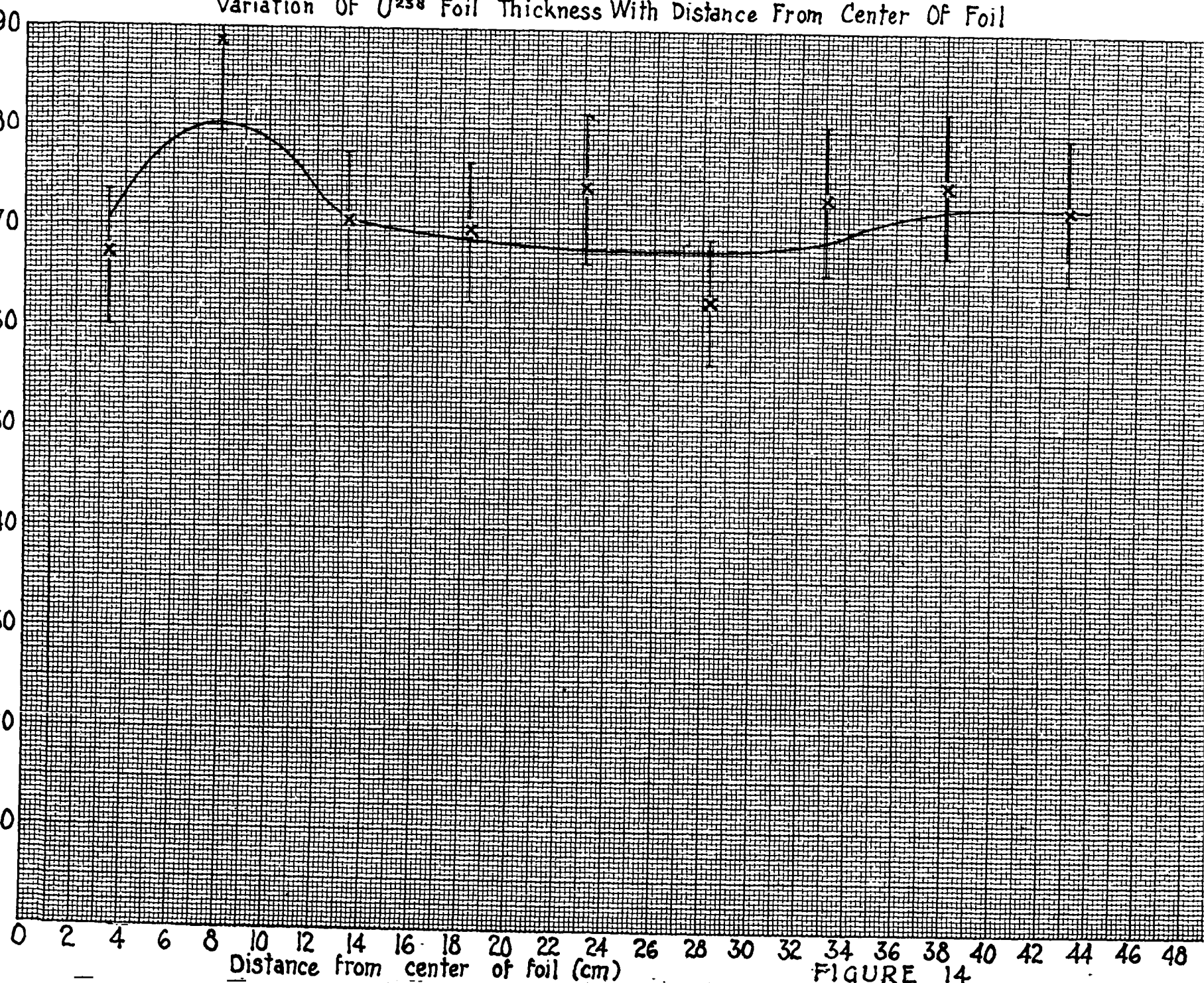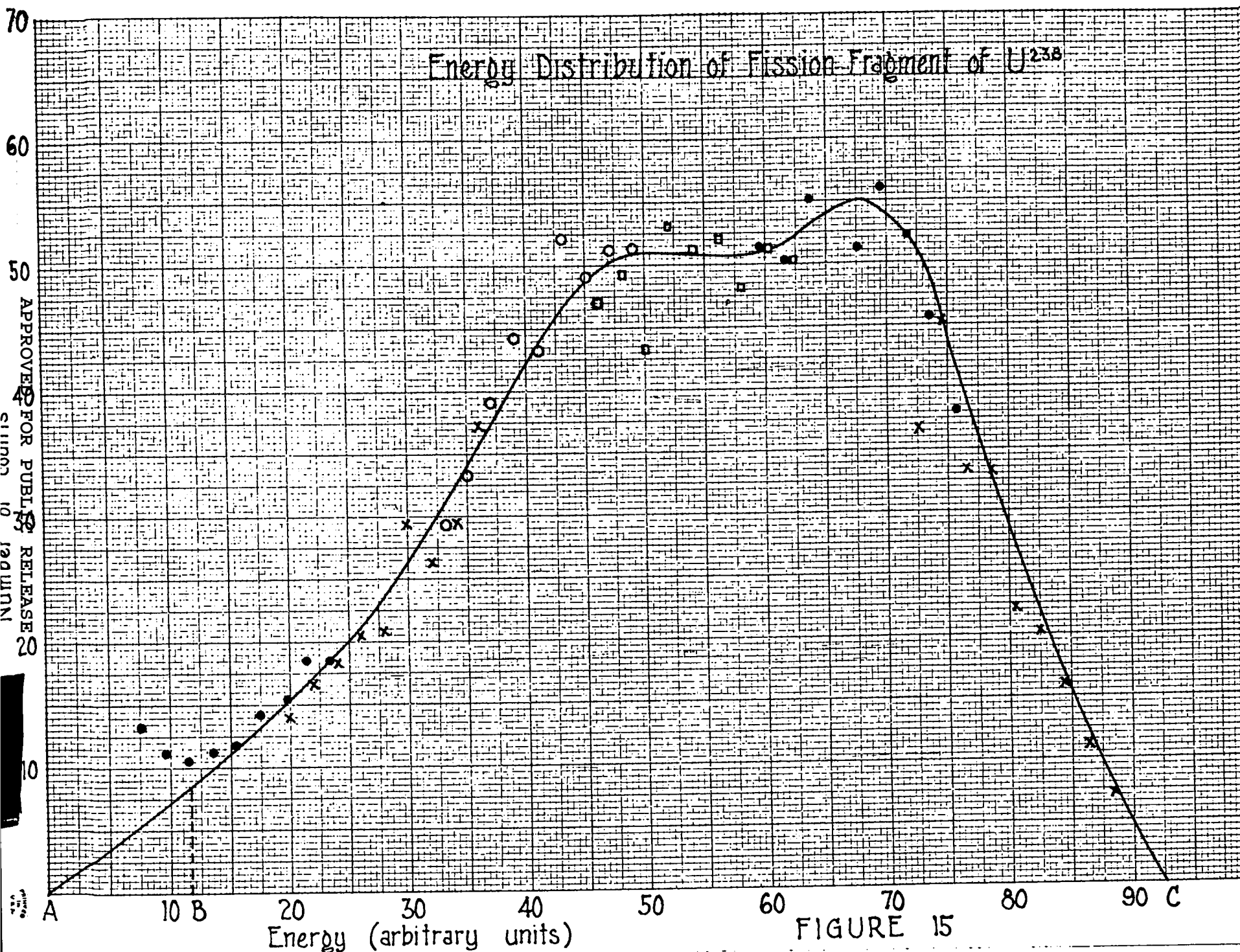Energy Distribution of Fission Fragment of U²³⁸

FIGURE 15

Energy (arbitrary units)

Even more important than an accurate determination of the uniformity of the U^{238} foils is the determination of the actual thickness of the U^{238} foils, since this enters directly into the equation for the cross section. The correction that must be made to the observed number of fissions can be divided into two parts: a correction for the fraction of fissions not observed because of complete absorption of the energy of the fragments of U_3O_8; and a correction for the fraction of the fissions not observed because the fragments which did penetrate the U_3O_8 did not have sufficient energy to overcome the bias setting. Now this latter correction is quite easy to make from Fig. 15. Since the bias setting was arbitrarily fixed at point B, the curve was integrated from A to B and from B to C. The number of observed fissions were then multiplied by $\dfrac{\int_A^B + \int_B^C}{\int_B^C}$ to give the number of fissions which occurred and yielded fragments which penetrated the foil. This correction amounted to only 2%. There still remains the determination of the absolute thickness of the foil and the total self-absorption, i.e., absorption which prevented fragments from penetrating the foil. It appeared that the simplest and most accurate procedure for making both determinations was to determine the "effective" thickness of the U^{238} for fission fragments,

i.e., F x total thickness where F is the fraction of all
fission fragments which are completely absorbed in the
U_3O_8. This was accomplished as follows: a determination
was made of the energy distribution of the α-activity
of each of the foils over an accurately determined area
in a Frisch-grid ionization chamber, utilizing the
10 channel discriminator. Fig. 16 is a plot of such a
determination. These curves were extrapolated to zero
and integrated to yield the total activity of each of
the foils. Since the specific activity of this U^{238}
sample was known to $\pm$ 0.5% this immediately gave the
effective thickness of the foils for particles of energy
4.75 Mev, i.e., the total thickness - F_1 x total thickness
when $F_1 =$ fraction of all alphas not counted because
they were completely absorbed in the U_3O_8. In order to
obtain the effective thickness for fission fragments it
was necessary to correct for the difference in range
between fission fragments and particles of energy 4.75
Mev. It has been shown by Rossi and Staub (LA-1004)
that the detection efficiency of a counter for α-particles
is found by

$$P\,(B) = 1/2 \left[1 - \frac{T}{2(R_0 - R_b)} \right] \tag{2}$$

where T = thickness of foil

R_0 = range of α-particles in the foil

Energy Distribution Of Alpha Particles From U^{238} Foil

Energy (arbitrary units)

FIGURE 16
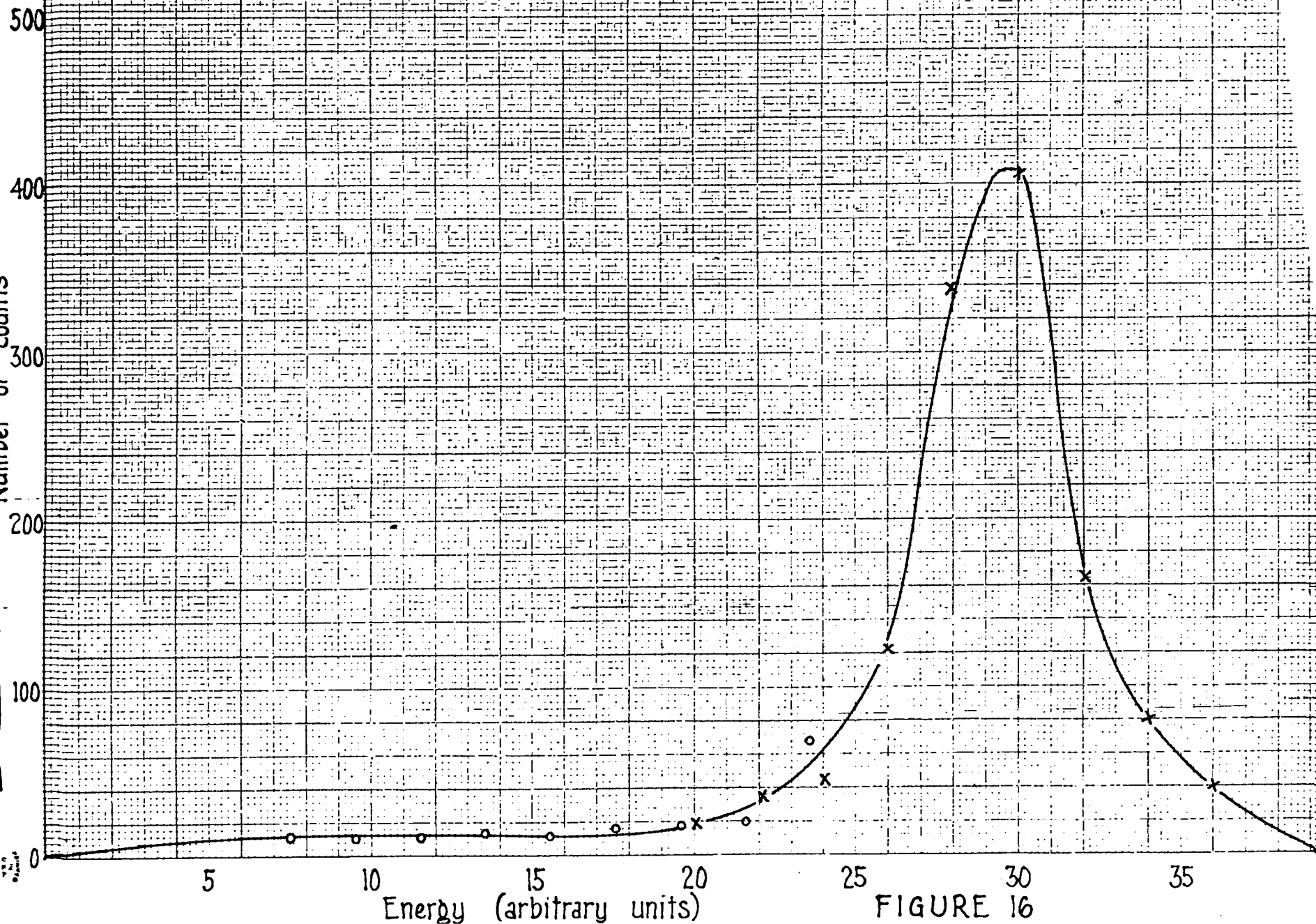
- 38 -

R_b = range of particles equal to the bias energy B
and $T \leq R_o$.

In our cases the bias energy B is zero since
we extrapolate all our curves to zero. We then have:

$$F(B) = 1/2 \left[1 - \frac{T}{2R_o} \right] \tag{3}$$

For fission fragments the formula is of course:

$$F(B) = 1 - \frac{T}{2R_o} \tag{4}$$

where R_o = range of fission particles.

With the aid of the above formulae and by taking
the mean range of fission particles to be 10 mg/cm^2
in U_3O_8 and the range of alpha particles of energy 4.75
Mev to be 11 mg/cm^2 in U_3O_8 a correction is obtained
which, when applied to the effective thickness of U_3O_8
for 4.75 Mev alphas, gives the effective thickness of
U_3O_8 for fission fragments. This correction is 0.4%;
i.e., the effective thickness of U_3O_8 for fission frag-
ments is thus 0.4% less than for 4.75 Mev alphas. The
effective average thickness of the U foils for fission
fragments then turns out to be 0.641 mg/cm^2 and it is
this value, multiplied by 12, which appears in the cross-
section formula given below as Eq. (6).

As a check on the method for determining the
thickness of the U^{238} from alpha activity, a foil was

counted and the U^{238} was then separated by R. W. Potter
using an ether extraction method. This uranium was then
weighed. The weight obtained in this manner coincided
with the weight deduced from the specific activity to
well within the accuracy of the chemical separation
method, which accuracy was about 5%.

An initial difficulty experienced in this
experiment concerned fissions produced in the fission
counter by background neutrons, i.e., neutrons arising
from reactions produced when deuterons strike either the
cyclotron dees, the sides of the cyclotron tank, the
beam collimating diaphragms or the target chamber windows.
It was found possible to eliminate practically all
neutrons with energy over the fission U^{238} fission
threshold by shielding the cyclotron tank proper with
water and paraffin. Also the slow neutrons which arose
due to this process outside of the shielding were not
sufficient to produce appreciable fissions in the small
amount of U^{235} contained in the U^{238} foils (U^{235} was
present to only 1 part in 3300). The background due to
the collimating diaphragms was considerably reduced by
making the diaphragm of gold. It was found that gold
has only about 0.3 the neutron background of brass, for
example.

The target chamber was originally used with

- 40 -

mica windows at all ports. The neutron background
was of course chiefly due to the front and rear windows
which had a combined thickness of about 5 mg/cm^2. It
was found during the course of the experiment that a window
of .0003" tantalum produces only 0.386 the neutron
background of a 2.5 mg/cm^2 mica window and a tantalum
window was accordingly substituted for the mica window
at the exit port of the target. The mica window was
retained at the entrance port on the basis of scattering
considerations.

Even after all the above improvements were
made, there were produced about 1000 background fissions
in the chamber for every fission produced by a neutron
in real coincidence with a He^3 entering the He^3 counter.

LA 710

VI. PROPORTIONAL COUNTER .

Fig. 17 shows the proportional counter used
in this experiment. It is of more or less conventional
design. Several special precautions were, however, taken
in order to eliminate possible α-particles which might
result from an n,α reaction in the glass insulator; a
shield of Poly T.F.E. was placed around this insulator.
All parts of the counter were also carefully decontaminated
in dilute HNO_3 before assembly.

The central electrode made of 10 mil Kovar
wire served as the high voltage and collection electrode,
the signal being taken off through a 5000 volt .0001 MF
condenser. The counter was operated with argon at pres-
sures ranging from 20 cm to 70 cm of Hg and at voltages
ranging from 500-2000 volts. The rise time of the pulses
was $\sim$ 1.1μs and the pulse width was $\sim$ 2-3 μs.

Fig. 18 is a family of gas amplification curves.
The counter was operated with a gas amplification of $\sim$10.

The resolution of the proportional counter
was determined by obtaining the energy distribution of
monoenergetic alphas produced by a thin plutonium foil
under the same conditions as prevailed during the count-
ing of He^3 particles, with the single exception that
there was only one mica window between the particles and
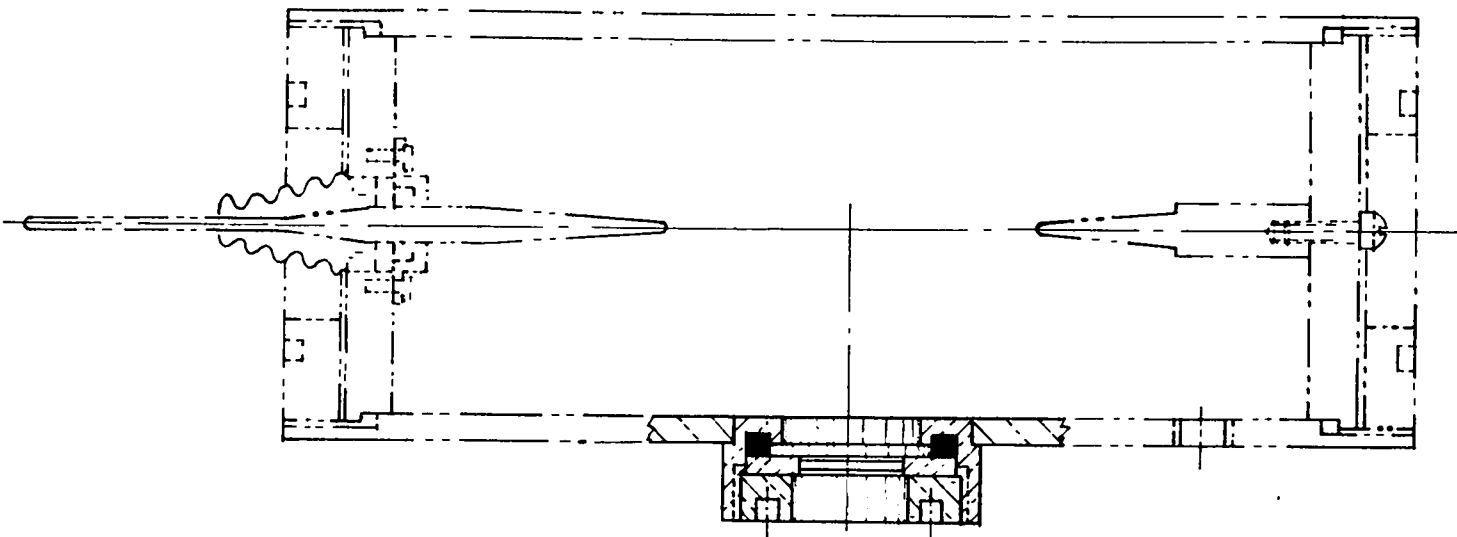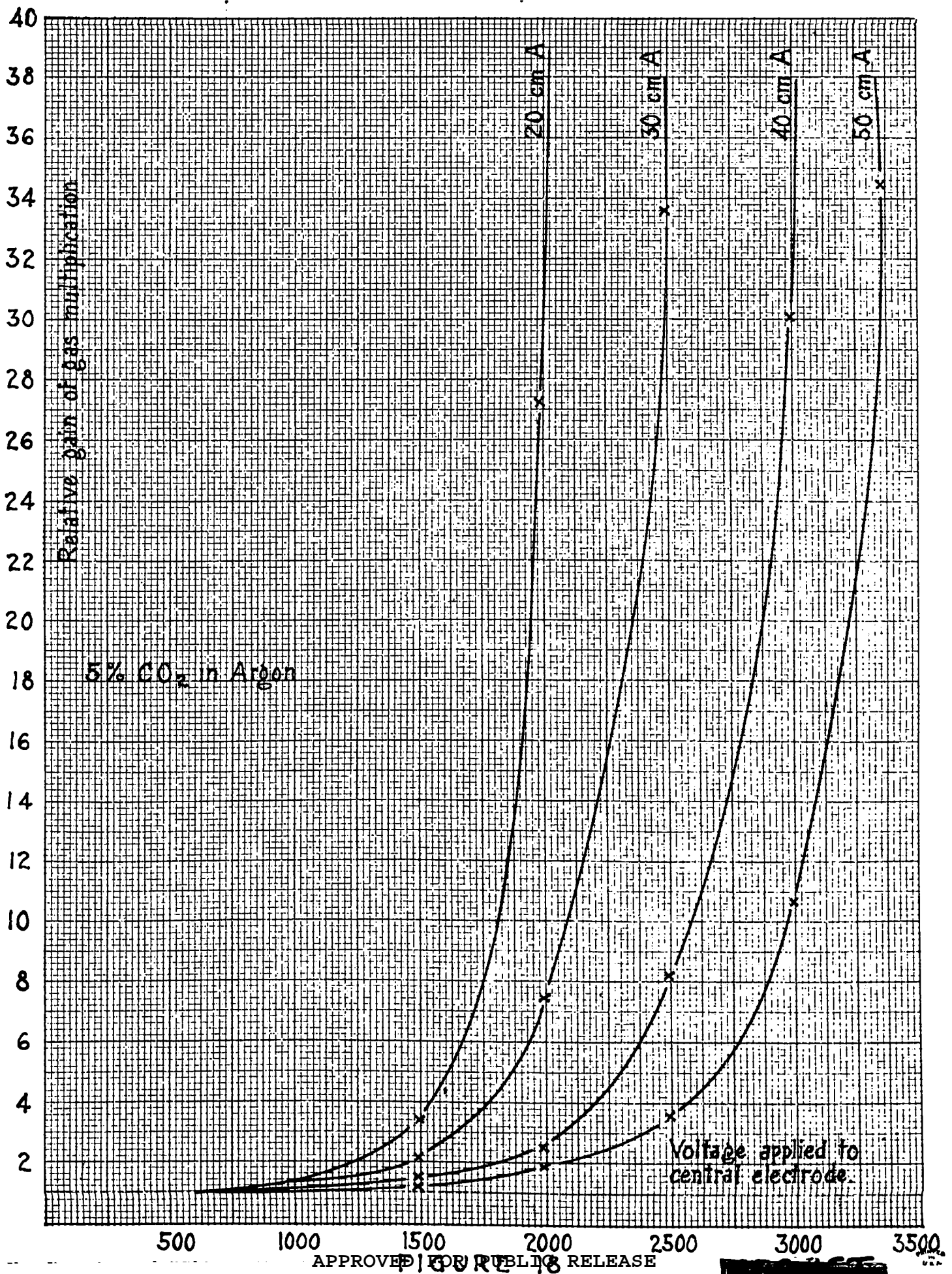the gas in the counter - namely, the counter window.

FIGURE 17

Proportional Counter

LA 710

- 44 -

Under these conditions the width at half-maximum of the energy distribution of the plutonium alphas was 3.5%.

A number of background difficulties were experienced when first the counter was tried. The background difficulties fell into two categories, gamma-ray background and particle background. The gamma background was sufficiently reduced by encasing the counter in 2" of lead. The other major source of background, that due to ionizing particles, resulted from deuteron reactions in the mica windows of the gas target which, during the initial set-up, the proportional counter was able to see and from recoil nuclei scattered by high energy neutrons. The former difficulty was successfully eliminated by use of the target arrangement shown in Figs.21 and 22. The latter difficulty, the considerable background produced by scattering of the large neutron fluxes produced by energetic deuterons upon being stopped, was sufficiently decreased by the methods described in the preceding section.

Another source of background consisted of voltage breakdowns inside the counter. These were almost completely eliminated by applying over-voltage on the counter and allowing it to "cook" for 5 minutes.

Since the He^3 particles essentially monitored our neutron flux, it was necessary to know that the

particles counted as He^3 particles did not include
scattered deuterons, protons, and tritons from the
$D(D,H^3)H^1$ reaction or recoil nuclei from the neutron
background. Since the rate of energy loss per cm
path of D, H^1, and H^3 particles is less than that of
He^3 particles, it follows that if one uses absorbers
(when necessary) in front of the proportional counter
and a pressure in the proportional counter such that the
He^3 particles are just stopped inside the proportional
counter, they will give up more energy and hence produce
higher pulses than any of the other particles mentioned
whether they be wholly or partially stopped in the chamber.
Since the energy of the He^3 particles at any angle with
respect to the deuteron beam could be calculated from the
deuteron energy and the Q of the reaction, it was possible
to always predict the amount of absorber necessary in
front of the proportional counter together with the amount
of pressure required in the counter to just stop the
He^3 particles inside the counter. These predictions were
in all cases borne out experimentally, which was an
additional criterion for establishing the fact that the
particles being counted were actually He^3 particles.
This permits one to bias against protons, deuterons, and
tritons. By making a background run with H^1 in the
target rather than D^2, it was determined that particles

of mass > 3 (for example argon recoil nuclei) gave
very few if any pulses in the energy region of the He^3
pulses, and even these background counts were corrected
for.

Fig. 19 shows the energy distribution of the
He^3 particles obtained from the $D + D \rightarrow He^3 + n$ reaction
using the above counter at 39.7° with respect to the
incident deuteron direction. Although the number of
He^3 particles counted served to define the number of
neutrons entering the fission counter and hence the
neutron flux, it was not necessary to count all He^3
particles entering the proportional counter. This fact
was taken advantage of by setting the bias at Point B,
for example, and counting all He^3's with energy greater
than this. By so doing, the background correction was
reduced to approximately 1%. In order to correct for
this background, the following procedure was used: The
background was appropriately extrapolated as shown by
the dotted line in Fig. 19. An aid to this extrapolation
in the higher energy region (from Point B up) was the
determination of the background with H^1 instead of D^2
in the target. A curve was then constructed of the number
of background counts/unit current vs. total counts per
unit current for a sufficient number of bias settings.
All runs were then corrected with the appropriate correc-
tion factor.

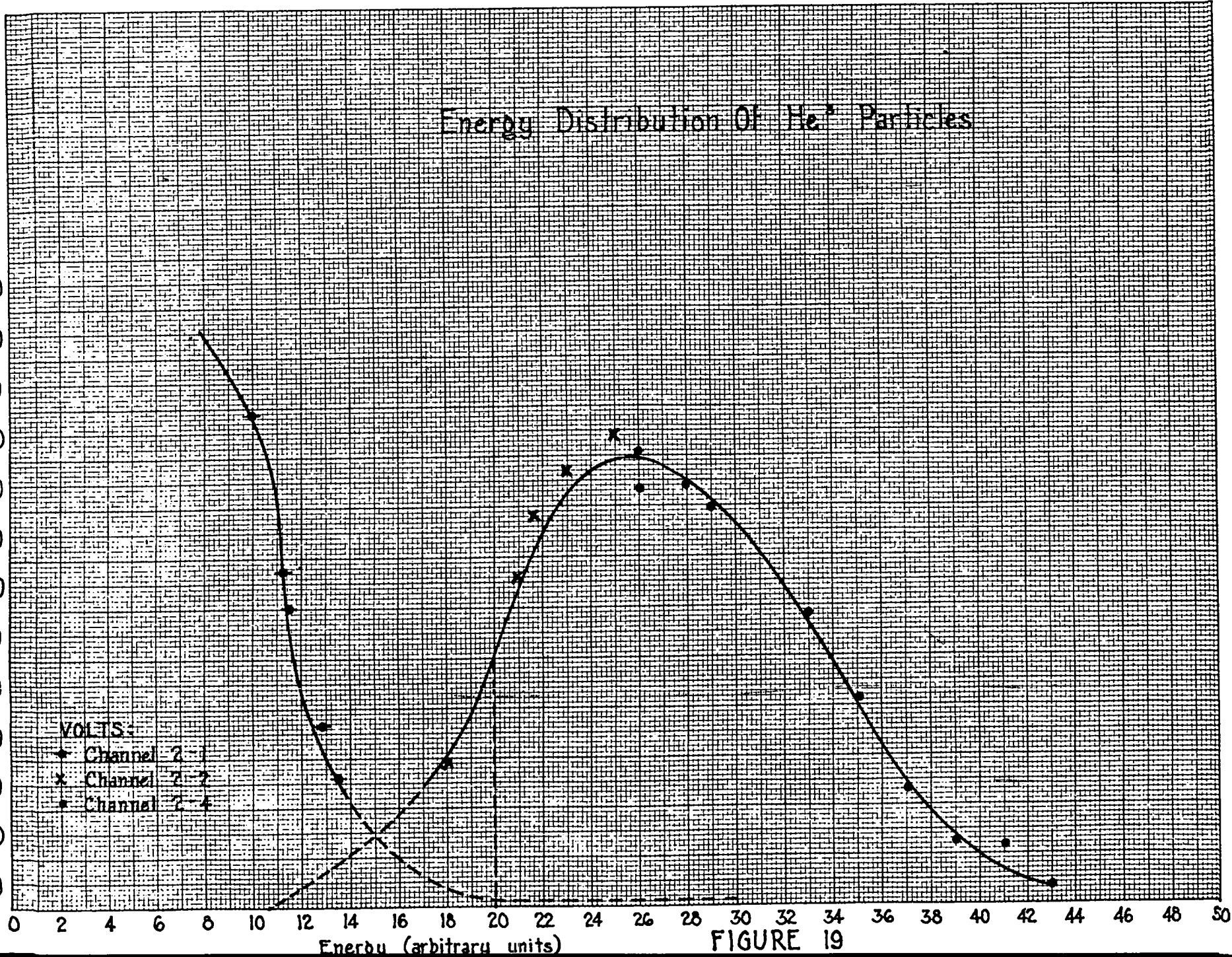Energy Distribution Of He³ Particles

FIGURE 19

- 48 -

It has now been shown how the three essentials of any cross-section measurement were accurately determined; namely, the flux of bombarding particles (in our case neutrons whose flux was determined by counting the coincident He^3 particles), the amount of material intercepting this particle flux and the number of reactions produced (in our case, this of course involved determining the number of fission particles liberated with energy sufficient to penetrate the foil of active material). The following equation determines the fission cross-section from these three quantities as determined from the above evaluations.

$$\frac{\text{No. of fissions}}{\text{Unit Time}} = \frac{F}{\text{Unit Time}} \times \frac{\sigma \times A \times n \times T \times 10^{-3} \times 6.023 \times 10^{23}}{238} \tag{5}$$

where the symbols have the following meaning:

$F =$ number of neutrons/cm^2 in coincidence with He^3's

$\sigma =$ cross-section per U^{238} nucleus

$A =$ average area of foils exposed to neutron beam

$n =$ number of foils

$T =$ average thickness in mg/cm^2 of U^{238} in foils corrected as outlined above.

Since $F = N/A$ where $N =$ total number of neutrons in coincidence with He^3's which enter the proportional counter

We have

- 49 -

$$\text{No. of Fissions} = \frac{N}{A} \times \frac{\sigma \times A \times n \times T \times 10^{-3} \times 6.023 \times 10^{23}}{238}$$

and

$$\frac{\text{No. of fissions} \times 238}{N \times n \times T \times 6.023 \times 10^{20}} = 5.14(\pm \sim 1.3\%) \times 10^{-20} \times \frac{\text{No. of real fissions}}{N}$$

(6)

where the number of fissions are given by the number of real coincidences corrected as outlined above and N is given by the number of He^3's counted, also appropriately corrected for background.

VII. NEUTRON ABSORPTION CORRECTION

Since only fission in coincidence with neutrons which are emitted in a collimated cone are counted, one does not have to worry about neutrons scattered into the counter by the walls of the reaction chamber, etc. However, it is necessary to correct for those neutrons in the defined cone which would have passed through the counter but which were absorbed or scattered out of the beam by the intervening material. Therefore, the walls of the targets and the scattering chamber in the path of the beam were milled down so that there was only 1/16" of brass and 1/8" of steel between the counter and the target gas. (Figs. 2, 3, 21, and 22). The absorption correction for this material and also the walls and plates of the fission counter was determined experimentally.

Absorption runs were made using the 10.5 min. activity of a $Cu^{63}(n, 2n)Cu^{62}$ detector. It had been shown previously that most of the activity of this threshold detector was due to neutrons from the $D(d,n)He^3$ reaction in the deuteron target. The background found by substituting hydrogen for deuterium in the target was about 10%. The experimental set-up is indicated in Fig. 20. This experiment gives absorption and inelastic scattering of neutrons from above the threshold
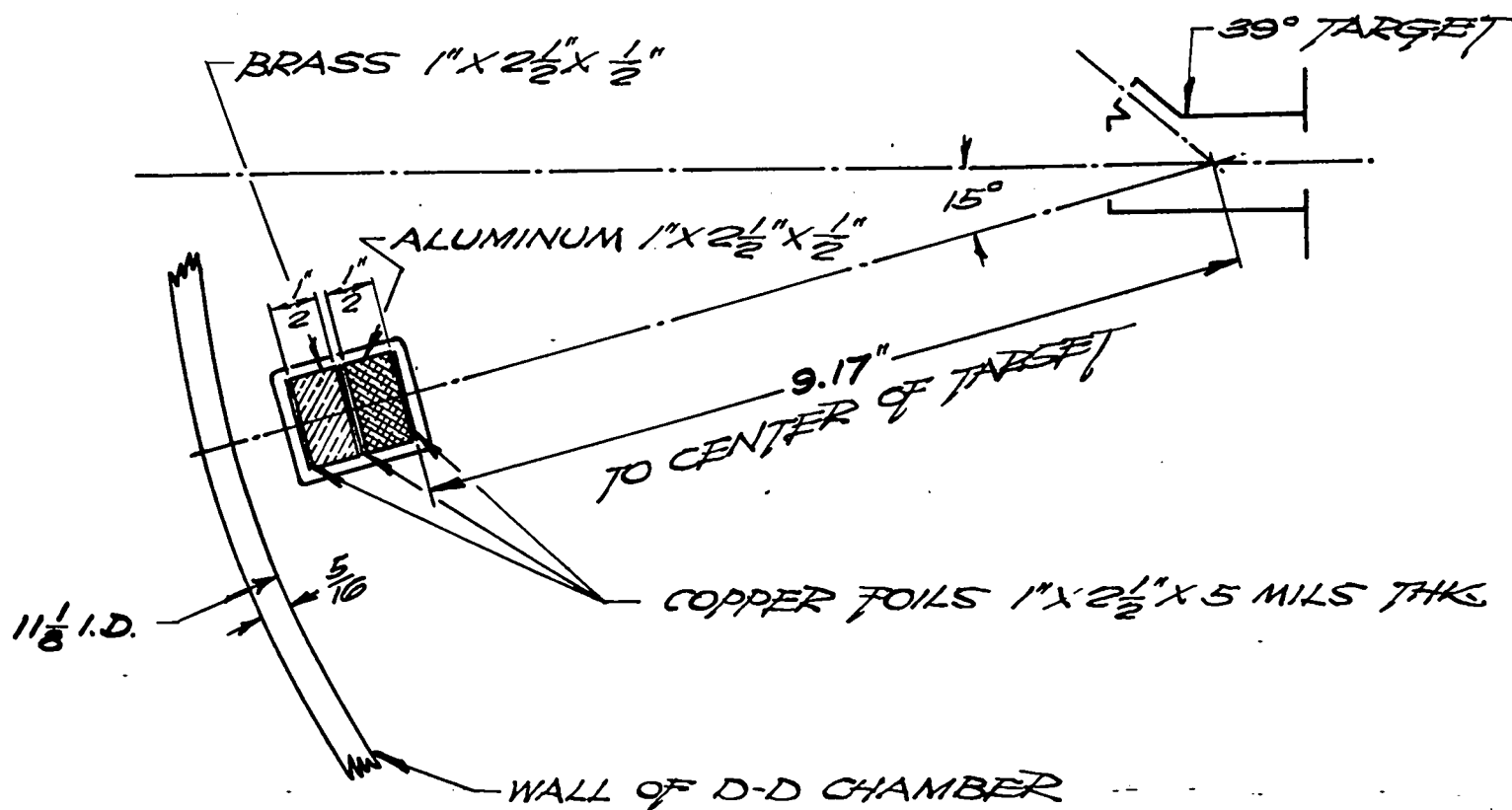
FIG. 20

SET UP FOR DETERMINING NEUTRON ABSORPTION CORRECTION

- 52 -

11<E_n<12 Mev. (A report on $Cu^{63}(n,2n)Cu^{62}$ reaction
is forthcoming). Copper foils 1"x2$\frac{1}{2}$"x5 mils thick
were used as detectors. The copper foils were sandwiched
between plates of the material, the absorption of which
was being studied. The group of absorber and foils were
covered by 30 mil cadmium to reduce slow neutron activity.
The front foils monitor the neutron beam. The ratio
between activity of the back foil and the foil in front
of any absorber gives the neutrons absorbed or scattered
from the beam by that absorber, after a slight correc-
tion for solid angle is applied. Second order corrections
due to neutrons back-scattered into the front foils were
not applied for the evaluation of this correction factor.

The deuterium gas of the targets was bombarded
for about 20 minutes by the cyclotron deuterons and then
the foils were removed and counted in glass-walled
geiger counters. Each sample was counted about 5 times
in each of three counters, so that 3 decay curves for
each sample were obtained. The 10.5 minutes activity
was well resolved. A summary of the results is in Table
I. The error is obtained from the spread in activities
of the three counters and hence is only the counting
error.

LA 710

TABLE I

Absorber	Thickness	N_b/N_f Activity Back Foil / Activity Front Foil	Absorption Factor = Log N_f/N_b
Brass	1/2"	.86 ± .02	.15 ± .02
Steel	1/2"	.87 ± .02	.14 ± .02
Aluminum	1/2"	.99 ± .02	.01 ± .02

One can make an estimate of the absorption factor for iron from data in the literature. The total cross-section for iron by transmission experiments is given as 2.8 ± 0.3 barns (Rev. of Mod. Phys. 19, #4, 275, (1947)). Since most neutrons scattered into the forward direction would be detected in our experiment, one should subtract the inelastic scattering in the forward direction from this value. A rough estimate of this scattering cross-section can be obtained from Barschall and Landenburg (Phys. Rev. 61, 129, 1942) which was measured at 2.5 Mev and is 0.9 ± .2 barns. The absorption factor calculated from these values

$$\left[2.8\ (\pm\ 0.3) - 0.9\ (\pm\ .2) = 1.9 \pm 0.4\right] \text{ barns is}$$

.20 ± .04, which is to be compared with our measurement of .15 ± .02. They agree within the limits of error, even though the estimates involve measurements made at somewhat different energies. Barschall and Landenburg also find that the absorption of aluminum is somewhat less than that from iron, in agreement with Table I.

- 54 -

The $Cu^{63}(n,2n)$ determination of absorption of
neutrons from the beam agreed within the limits of error
with a determination which was made using the fission
counter as a neutron detector. This experiment involved
taking runs on the real coincidence fissions per He^3
particle with and without additional absorbers being
present. The statistical errors and other errors were
too large, however, to warrant using this latter method
to evaluate the absorption correction.

Using the data given in Table I, one can cal-
culate the neutron absorption correction which must be
applied to the data to obtain the U^{238} cross-section.
Table II gives the thickness of each material between
the neutron source and the average plate of the fission
counter during the runs for the determination of this
cross-section.

<center>TABLE II</center>

Material	Thickness	$\overset{A}{\underset{}{\text{Absorption Factor from}}}$ Table I
Steel	.125"	.035 $\pm$ .005
Brass	.076"	.023 $\pm$ .003
Aluminum	.312"	.006 $\pm$ .012

$$\Sigma\, A_i = .064 \pm .013$$

This indicates about a 6% correction must be
applied to the data to allow for neutrons absorbed or
scattered out of the beam.

- 55 -

VIII. **EXPERIMENT**

The procedure followed in preparing for and carrying out the determination of the cross-section at a certain neutron energy is as follows:

A. Install and line up the suitable gas target.

B. Determine the spread and position of the deuteron beam.

C. Determine the energy of the deuteron beam.

D. Install suitable diaphragms in the proportional counter and target and line up the fission counter.

E. Calibrate amplifiers, etc.

F. Adjust proportional counter voltage and/or gain to give to give correct amplitude He^3 peak.

G. Make runs of about 1/2 hour duration and record fissions, He^3's counted, and coincidences.

H. Make runs for resolving time determination.

I. Repeat energy measurements from time to time.

A. The gas targets used in this experiment are illustrated in Fig. 21 and Fig. 22. Table III gives the thickness of mica on the windows used to obtain each point. A gold diaphragm 30 mils thick with a 0.466" diameter hole is fastened in front of the target to

Gold diaphragm

Mica

Beam →

Mica or Tantalı

39°

He 3

Mica
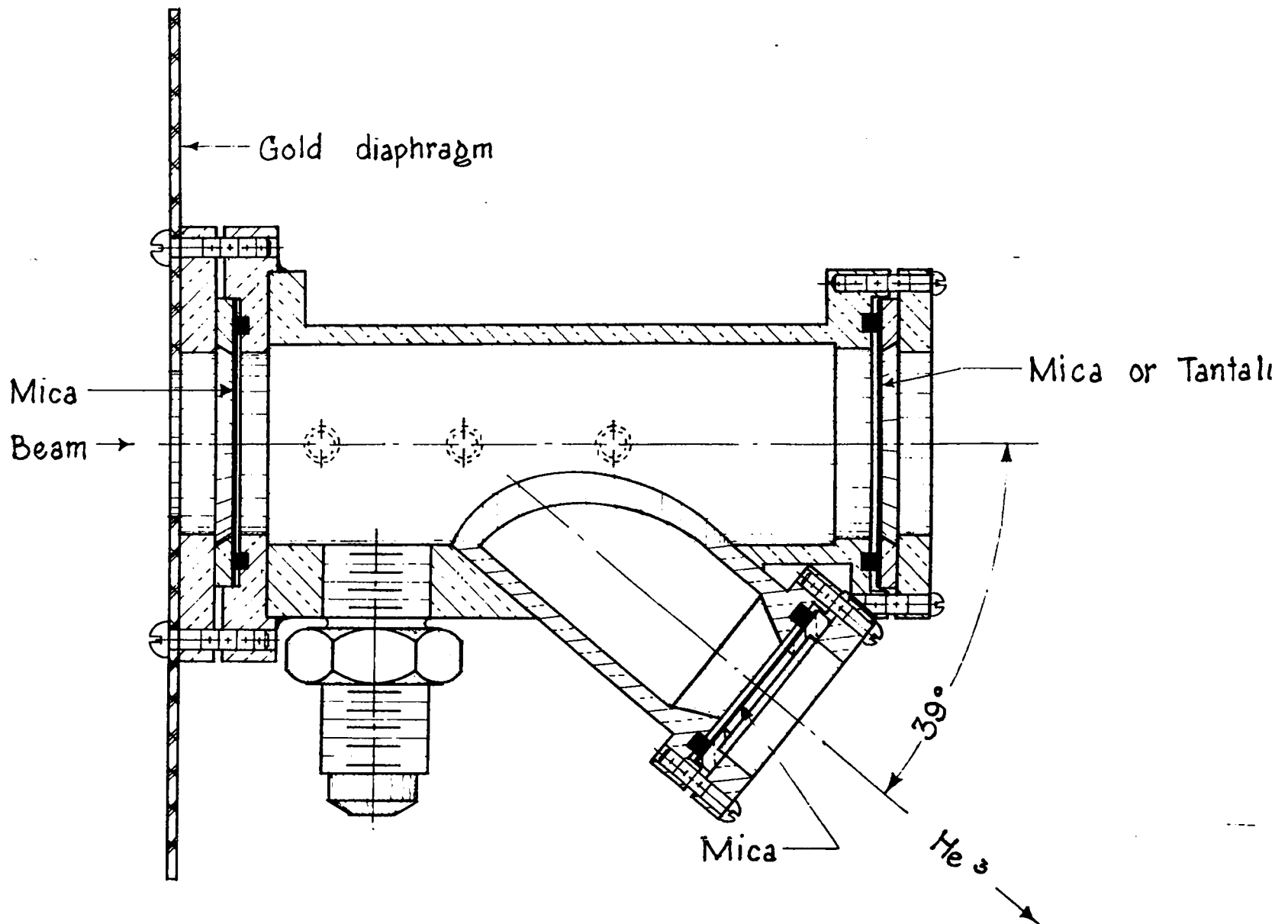
$$39° \text{ GAS TARGET}$$
$$\text{FIGURE 21}$$

|← 1" →|

Scale

GOLD DIAPHRAGM

$\frac{1}{16}$

BEAM

MICA

MICA

30°

H₂

|← 1" →|
Scale
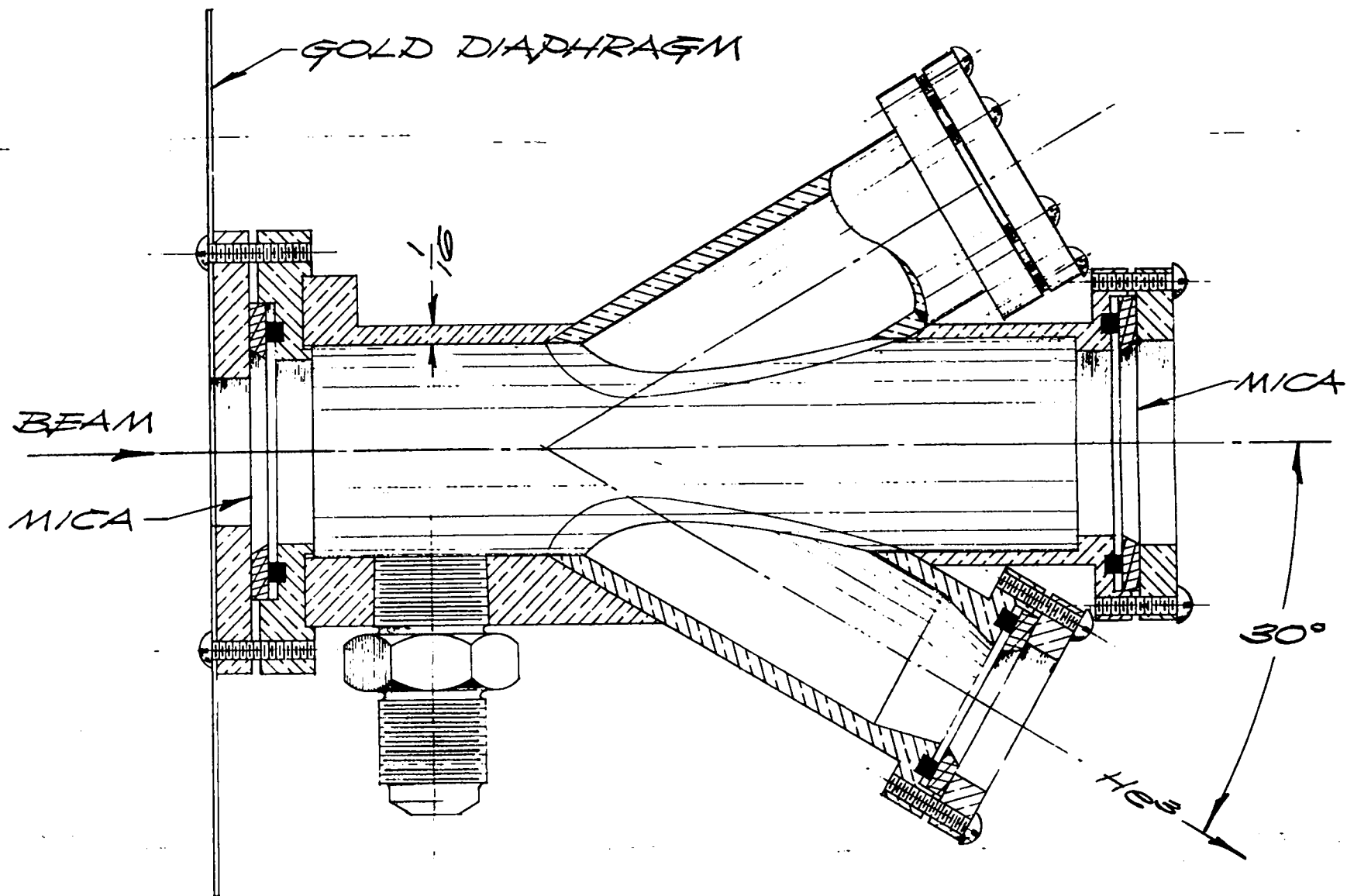
30° GAS TARGET
FIG. 22

SERIES	ϕHe^3	DIAPHRAGMS FOR He³ PARTICLES		THICKNESS OF WINDOWS IN TARGET			ENERGY OF DEUTERON BEAM MEV	HORIZONTAL SPREAD He³ BEAM $\Delta\phi He^3$	VERTICAL SPREAD He³ BEAM $\Delta\phi He^3$	CENTER OF NEUTRON BEAM ϕn	HORIZONTAL SPREAD NEUTRON BEAM $\Delta\phi n$	VERTICAL SPREAD NEUTRON BEAM $\Delta\phi n$
		TARGET	PROPORTIONAL COUNTER	ENTRANCE	EXIT	He³ PORT						
1	40.7°	3/16"x3/8"	3/16"x3/8"	2.82 mg/cm² mica	2.60 mg/cm² mica	1.30 mg/cm² mica	10.20	±2.28°	±3.8°	55.6°	±5.7°	±4.8°
2	29.7°	1/8"x1/4"	1/8" Dia.	2.60 mg/cm² mica	2.2 mg/cm² mica	2.0 mg/cm² mica	9.86	±2.10°	±2.3°	82.3°	±5.0°	±4.6°
3	39.7°	5/32"x3/8"	3/16"x3/8"	2.7 mg/cm² mica	.0003 mil Tantalum	1.4 mg/cm² mica	10.75	±2.15°	±3.80°	56.90°	±5.3°	±4.8°

TABLE III

LA 710

limit the beam. After installing the windows and testing them under pressure, one lined up the target. The back plate, slits, and Faraday cage were removed from the energy measuring section so that one could sight a telescope along the 0 - 180° reference line of the D-D chamber, as established by dropping a plumb bob from the graduated ring (Fig. 4). The target was moved on its platform and rotated until it was lined up on the line of sight. By use of a surface guage the height of the target was adjusted to that of the beam, which came 5-23/32" above the base of the chamber. It was estimated that the alignment could be accomplished to about 1/64".

B & C. The procedure followed in determining the spread and position of the beam has been described in Section II. The maximum angular spread of the beam was limited to $\pm 0.63°$ by a gold diaphragm in the 6" tube from the focus magnet. The energy of the deuteron determination has also been described in Section III.

D. From the energy and angular spread of the beam one calculates the diaphragms for the proportional counter and He^3 exit tubes of the target so that the associated cone of neutrons falls well within the U^{238} foils of the fission counter, the last foil of which subtends a cone of total included angle of 12.1°. The results of these calculations are given in Table III.

- 60 -

By having the cone of neutrons somewhat smaller than the cone of the fission counter, one can allow for small errors in aligning the equipment and in measuring the deuteron energy. For example, a 2% shift in deuteron energy corresponds to a shift of the neutron angle by 0.36° when the He³ angle is 39°.

Next, the center of the fission counter is lined up on the correct angle corresponding to the angular setting of the proportional counter. This is done by establishing a line with a straight edge which is directly over the calculated angle as determined by the graduated ring within the D-D chamber. When the fission counter is rotated to the correct position the reading of the angular scale on the track is taken. Thus, for each setting, the track is calibrated against the graduated ring. By use of a straight edge and a scale, the height of the fission counter is adjusted to be the same as that of the target and proportional counter. The angular settings of the fission counter together with that of the proportional counter for the various series of runs is given in Table III.

The calibration of the amplifiers and adjustments of the discriminator bias of the coincidence circuit are described in Sections V and VI. Before a run or series of runs one checks and records the gas

LA 710

pressure in the target, the proportional counter, and
the fission counter. Then the high voltage to the counters
is switched on. With a cyclotron beam one adjusts the
high voltage for the proportional counter to give the
He^3 pulses of the desired amplitude as described in
Section VI.

G. Now one is ready for the experiment. After
a fairly steady cyclotron beam is obtained, one records
the readings of the proportional counter scaler, the
fission scaler, the coincidence scaler, and the current
integrator scaler, together with the time at which
the electronic apparatus is switched on. The beam is
held as steady as possible for 1/2 hour and the experi-
mentor records any intervals of time the beam is off.
This off time is added to the length of the run at the
end. At the end of 1/2 hour of beam the time and the
readings of the above scalers are again recorded.

H. From time to time, the resolving time
of the coincidence circuit is determined experimentally.
Runs of 1/2 hour duration are made similar to the one
described above, except that the fission counter is ro-
tated to such an angle that no neutrons associated with
the He^3 particles can pass through it. Since for such
runs all coincidences are accidental, one can calculate
the resolving time from the simple relationship.

$$Ca = \frac{(N_{He3})(N_f)(\Delta T)}{\Delta t} \tag{7}$$

where $Ca =$ accidental counts obtained during interval

   $N_{He3} =$ He^3 counts obtained

   $N_f =$ fission counts obtained

   $\Delta T =$ resolving time

   $\Delta t =$ time of observation.

Since the accidental rate is determined by such runs spaced between the real runs, variations of cyclotron beam, etc., should average about the same for both sets of runs, so that the evaluation of the accidental counts during the real runs should be rather valid. The experimentally determined resolving times for all series of runs are recorded in Table IV.

TABLE IV

Series	E_n Neutron Energy Mev	τ Experimental Resolving Time (sec)	C_r/N_p			$\sigma_{2\theta}$ Barns
			Average of Series	Corrected for Neutron Absorption	Corrected for Fission Counter Bias	
1	8.8 ± 0.5	$2.23 \pm .12 \times 10^{-6}$	$20.8 \pm 2.0 \times 10^{-6}$	$22.2 \pm 2.2 \times 10^{-6}$	$22.7 \pm 2.2 \times 10^{-6}$	$1.17 \pm .11$
2	5.8 ± 0.4	$1.87 \pm .09$	12.1 ± 2.5	12.9 ± 2.7	13.2 ± 2.7	$0.68 \pm .14$
3	8.9 ± 0.5	$1.90 \pm .12$	18.7 ± 2.3	20.2 ± 2.4	20.2 ± 2.4	$1.04 \pm .12$

RESULTS

Each series of runs required about 15 separate runs of 1/2 hour each. The deuteron beam current was so adjusted as to give about equal number of real coincidences and accidentals. The data for this series of runs is given in Appendix III. Figs. 23, 24, and 25 show graphically how the number of real coincidences per He^3 particles for the sequence of runs varies. The points are plotted in the order in which they were taken. The represented error is calculated from the counting errors of the total coincidences and that of the accidentals. Thus, the quantity plotted for a run of Δt duration in which there are C total coincidences, N_{He^3} He^3 counts, N_f fission counts is

$$\frac{Cr}{N_{He^3}(corr)} = \frac{C - \frac{(N_{He^3})(N_f)\Delta\mathcal{T}}{\Delta t}}{N_{He^3}(corr)} \pm \frac{\sqrt{C + \frac{(N_{He^3})(N_f)\Delta\mathcal{T}}{\Delta t} + \left(\frac{N_{He^3} N_f \epsilon\mathcal{T}}{\Delta t}\right)^2}}{N_{He^3}(corr)}$$

(8)

where $\Delta\mathcal{T}$ is the resolving time and $\epsilon\mathcal{T}$ is its standard error as determined from the runs on resolving time. That the data and the errors are statistically significant is indicated by the way the points fall around their mean. About 2/3 of the points lie within their standard error of the mean in agreement with the principles of

Series #1
En = 8.8 Mev

FIGURE 23

FIGURE 24

Av 12.1 ± 2.5

Series #2
En ~ 5.6 Mev

Cr/Np corr

Run #

APPROVED FOR PUBLIC RELEASE

FIGURE 25

Series #3

$E_n = 8.9$ Mev.

Av 18.7 ± 2.3

LA 710
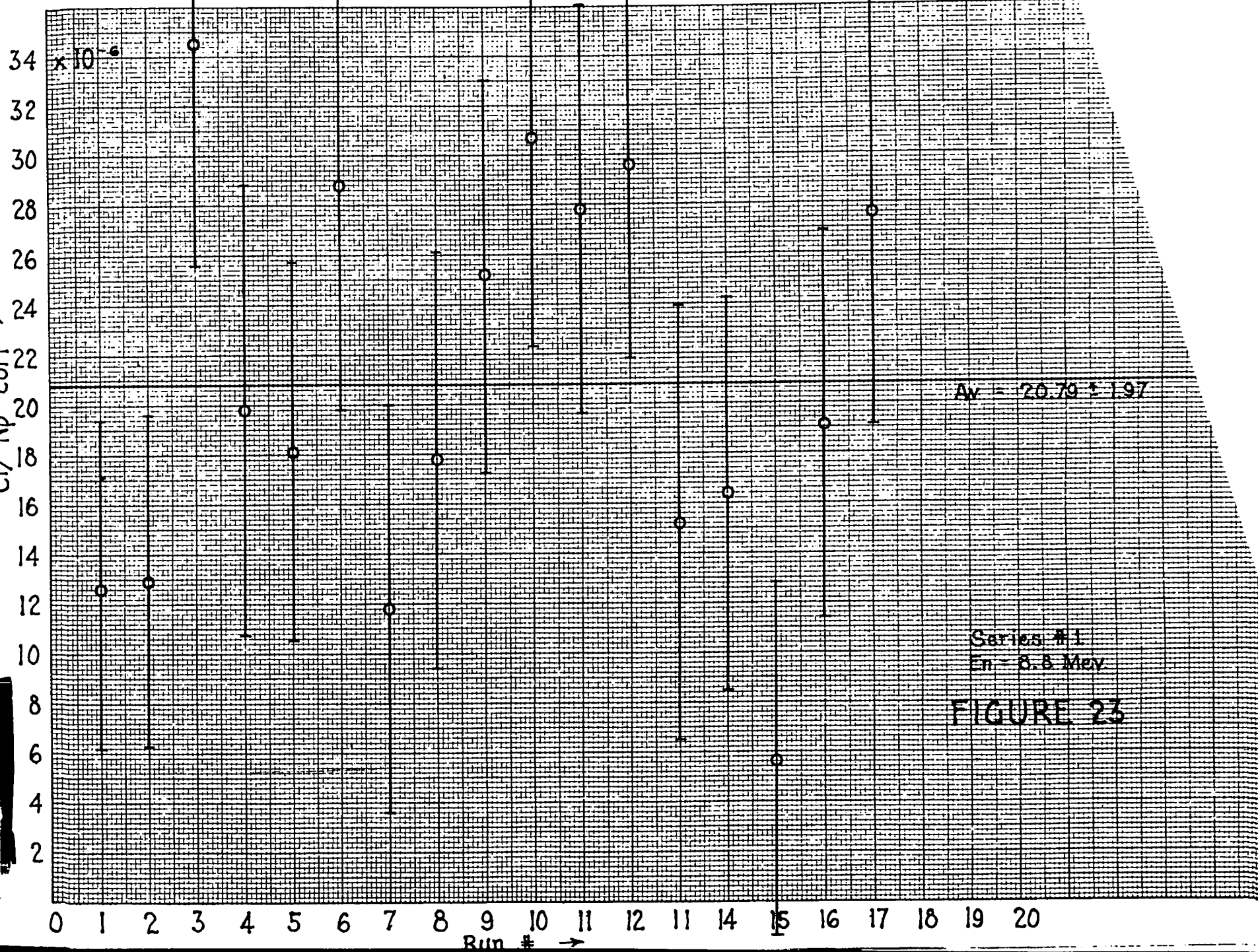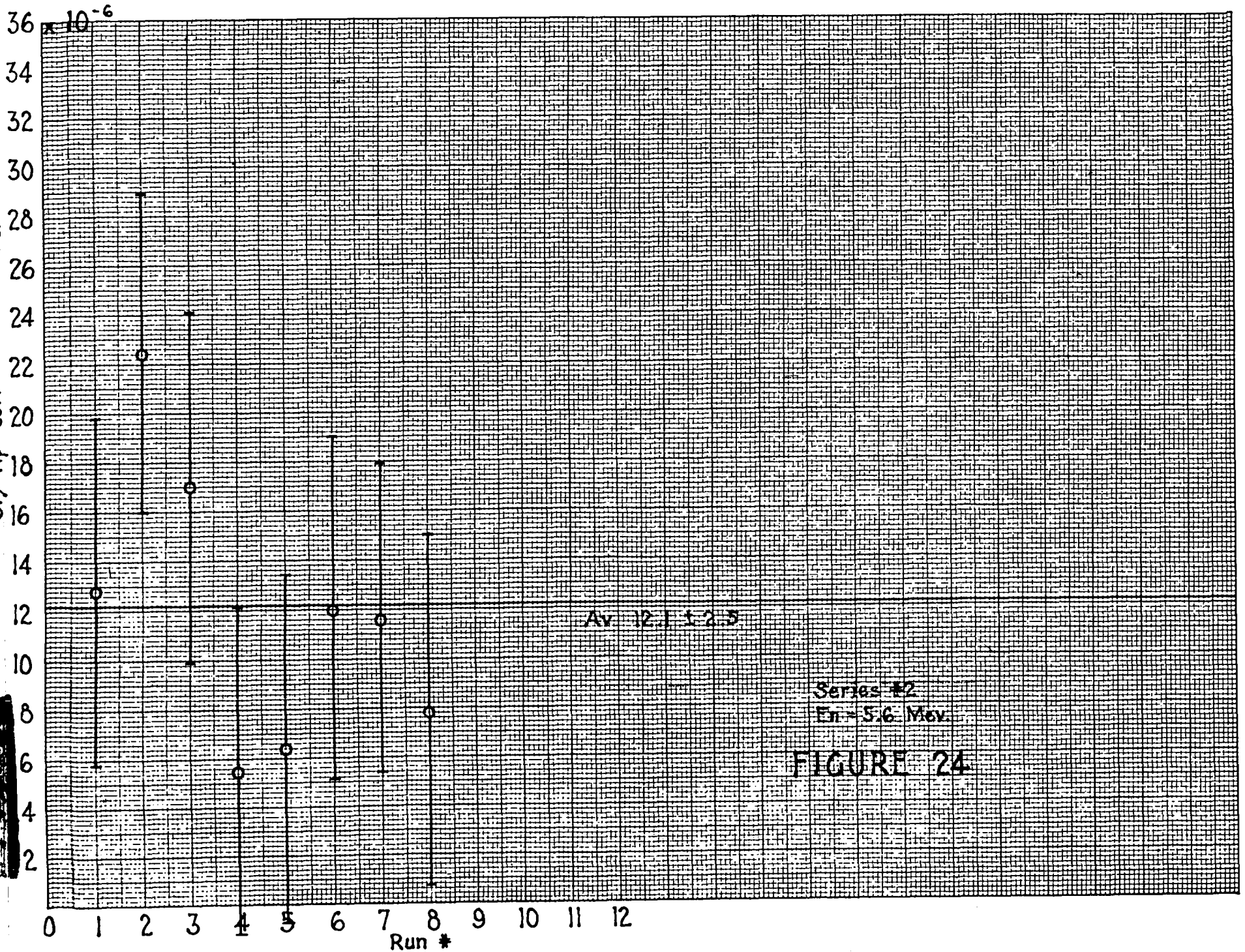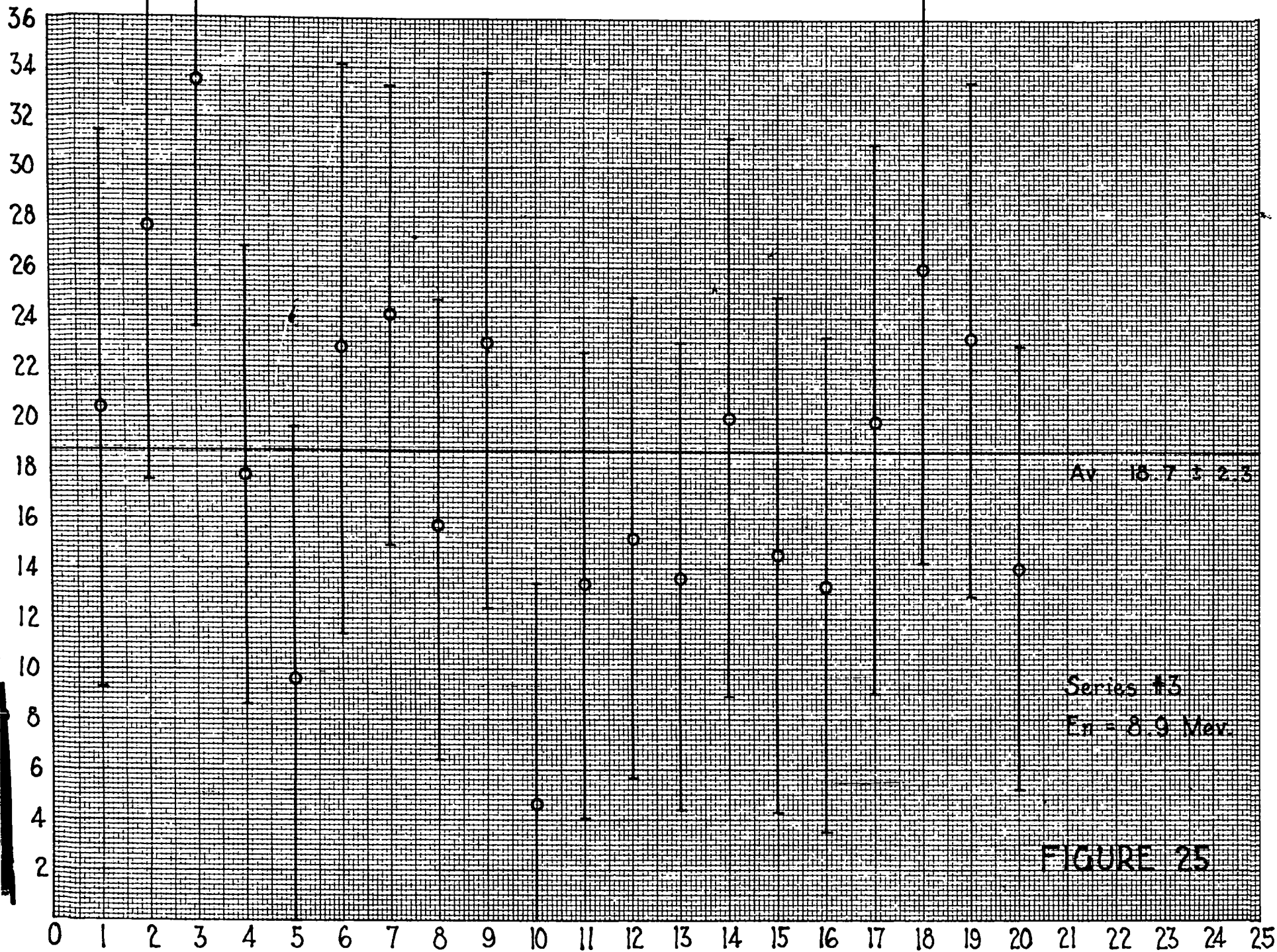
probability. The data does not indicate a significant
trend with order or runs.

As an example of the calculation of the result
of a 1/2 hour run, consider the data for the first
point of Fig. 25. From Appendix III, Series 3, the
recorded data was as follows:

$\Delta t =$ length of run $= 30$ min.

$N_f =$ fission counts $= 32,350$

$N_p =$ He^3 proportional counts $= 752000$

$C =$ coincidences counts $= 41$

Using Equation (7) and the resolving time for Series
#3 runs (TABLE IV) which is $\Delta T = 1.90 \pm .12$ µs one has

$$C_a = N_{He^3} \, N_f \, \frac{(\Delta T)}{\Delta t} = 25.7 \pm 5.2$$

where the error is essentially the square root of the
number of accidental counts. This is increased slightly
by the error of the resolving time.

The real coincidences then are:

$$C_r = C - C_a \pm \sqrt{C + \mathcal{E}_a^2} = 15.3 \pm 8.3$$

By the method described in Section VI it had been deter-
mined that for this run a fraction (.994) of the counts
of N_p are due to He^3

So $N_{He^3} = 0.752 \times 10^6 \times 0.994 = 0.748 \times 10^6$

Thus:

$$\frac{C_r}{N_{He^3}} = \frac{15.3 \pm 8.3}{0.748 \times 10^6} = \left(20.4 \pm 11\right) \times 10^{-6}$$

TABLE IV gives a summary of the data. Column 2 shows the average energy of the neutrons. The spread in energy corresponds to the width at half maximum of the energy distribution curve, and is derived from considerations of the angular spread of the He^3 due to finite width of slits and the angular spread and the energy spread of the deuteron beam. Column 4 is the mean value of the determination of the ratio of real fission coincidences per He^3 particles as taken from the data in Figs. 23-25. In Column 5, this ratio is corrected for neutron absorption by dividing by ϵ^{-A} where A is the absorption correction as discussed in Section VII. In Column 6, the data is corrected for the finite thickness of the U^{238} deposited on the foils of the fission counter as described im Section V. Column 7 gives the cross-section in barns after all corrections are applied.

In Fig. 26, the data discussed in this paper are plotted together with other determinations of fission cross-sections of U^{238}. Below 3 Mev the cross-section has been well established by a number of investigators (LA-520). The new value at 5.6 Mev agrees with previously determined values by the long electrostatic

BELOW 3 MEV ⎫
□   ⎬ LA 520
△   ⎭
⊖—CYCLOTRON, PRESENT DATA
▢ VAN DE GRAFF, L.A.M.S. 777
✕ L.A.M.S. 396
◆—COCKROFT-WALTON, PRELIMINARY

$\sigma_{(26)}$ BARNS

E_n (MEV)

- 70 -
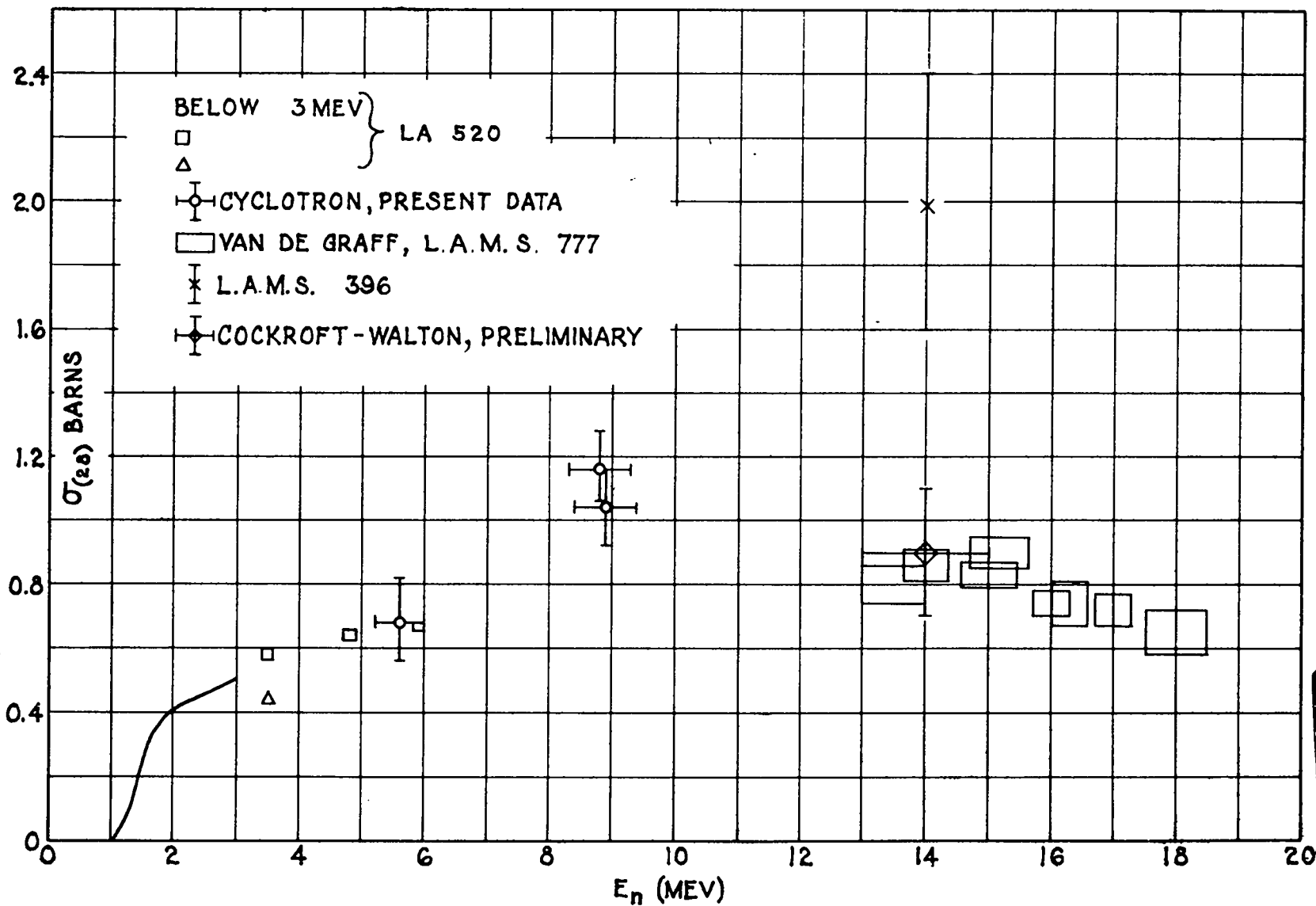
Fig. 26

generator. The new values at 8.7 and 8.9 Mev check each other and indicate that the cross-section is somewhat larger in this region than was previously supposed.

- 72 -

APPENDIX I

The details of the derivation of the energy equation are found in Creutz and Wilson's report. The procedure used in this experiment is as follows. Neglecting the relativity correction it is possible to rewrite the energy formula as

$$\frac{2M_0 \, c^2 \, W}{c^2 \, A^2} = \left[1 + \left(\frac{a + b/2 \, (1 - c^2 A^2/8M_0 c^2 W)}{D} \right)^2 \right]$$

Or

$$k(D) = 1 + \left(\frac{a + b/2 \, (1 - 1/4k(D))}{D} \right)^2$$

Expanding:

$$k(D) = 1 + \left(\frac{a + b/2}{D} \right) - .1532 \, \frac{1}{1 + \left(\frac{a + b/2}{D} \right)^2} + \cdots \tag{9}$$

Thus $k(D)$ may be found for any given value of D.
The energy is then given as

$$W \, (\text{Mev}) = Ck \, (D) \, (\Delta I)^2 \tag{10}$$

where C is a constant $= 87.55$.

A sample family of curves is attached. The correction for a given galvanometer deflection for the zero field is given in Chart I.

Let us assume that the measured values were

- 73 -

████████

$D \cong 16.4$ cm

$\triangle I \cong 113.05$ milliamperes $+ 1$ cm reading on the
galvanometer

Residual field (180° turn of flipcoil) $\cong$ 8cm.
Then $\triangle I$ corrected would be $113.05 + 1.6$ milliamperes
or 114.65 ma.

From Chart I we obtain the deflection correction
d_θ to be 0.7 cm and the current correction to be 5
milliamperes. The final value of D is $16.4 + 0.7$ or
17.1 cm and $\triangle I \cong 114.65 + 5.0 \cong 119.65$ milliamperes.

From Chart II we find for these values an
energy of 10.34 Mev. Applying the relativity correction
which amounts to approximately 0.3% in the region, the
final value of the energy is 10.31 Mev. This value
must be corrected for target gas and windows in order
to obtain the energy at the desired point where the
deuterons intersect the exit cone to the proportional
counter.

It should be noted that if the values a or
b are changed a new family of curves must be drawn. If
w, the width of the rectangular flux coil, is changed, a
new value of constant C must be determined.

████████

Procedure

1° Add do to deflection as measured.

2° Add ΔI_0 to $\Delta I \pm \frac{\text{scale cm deflection}}{3.5} \times 5.6$ md.

3° Read energy on chart II.

4° Add correction for mica window and De gas.

5° Add correction for relativity at 10 mev = 0.026 mev.

ΔI_0

do

Galvanometer deflection for
180° turn of flip coil

Scale cm

10

9

8

7

0.6

0.8

do (cm)

CHART III

APPENDIX II

LA 710
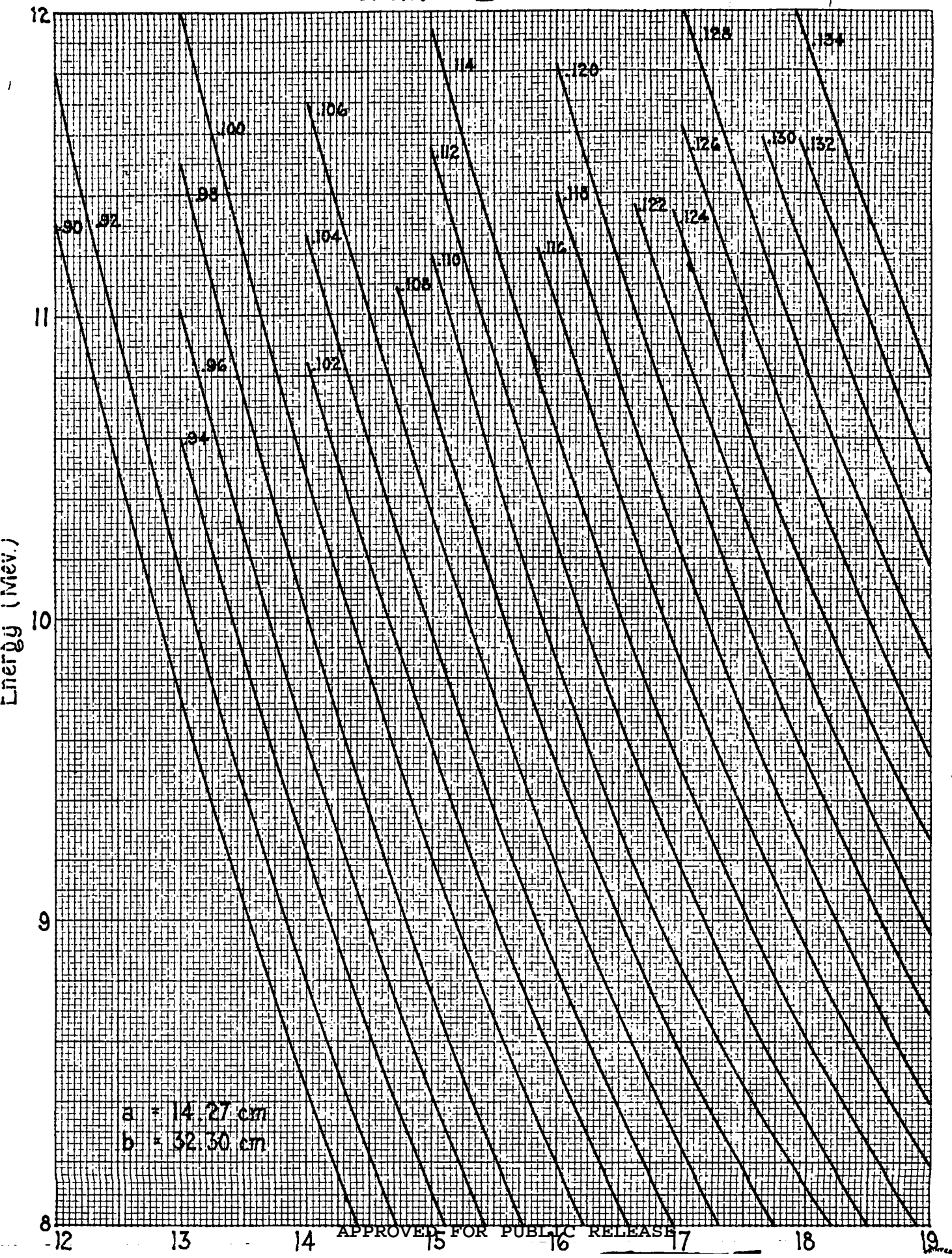
Date	Series No.	D cm	ΔI_c ma	E Mev	E Ave.	E_c
2-16-48	1	17.81	124.01	9.92	9.99	10.12
		17.66	123.75	10.04		
		17.61	122.96	9.94		
		17.61	121.81	9.92		
		17.44	122.42	10.00		
		17.41	121.73	9.95		
		17.31	121.61	10.08		
		17.31	121.96	10.10		
2-20-48	1	17.31	122.58	10.10	10.04	10.19
		17.34	122.33	10.12		
		17.36	127.60	9.98		
		17.36	121.14	9.94		
2-23-48	1	17.76	126.24	10.28	10.17	10.30
		17.71	125.30	10.16		
		17.71	124.91	10.13		
		17.53	124.53	10.18		
		17.48	123.79	10.10		
3-1-48	1	17.64	123.83	10.01	9.97	10.10
		17.44	123.01	10.00		
		17.39	122.80	9.99		
		17.39	122.04	9.89		
2-25-48	1	19.00	131.96	10.25	10.17	10.31
		18.85	132.47	10.21		
		18.85	131.28	10.05		
3-22-48	2	18.01	123.01	9.47	9.51	9.80
		17.95	122.67	9.52		
		17.90	122.51	9.52		
		17.90	122.43	9.52		
3-25-48	2	18.00	124.44	9.78	9.75	9.98
		17.95	124.41	9.78		
		17.95	124.00	9.68		
		17.83	124.00	9.74		
3-31-48	2	18.10	123.77	9.55	9.64	9.80
		17.65	121.34	9.58		
		17.45	119.96	9.58		
		17.25	119.62	9.70		
		17.20	119.76	9.79		

(continued)

APPROVED FOR PUBLIC RELEASE

- 77 -

(Appendix II, cont'd)

LA 710

Date	Series No.	D cm	ΔI_0 ma	E Mev	E Ave.	E_0
6-15-48	3	16.55	120.24	10.54	10.55	10.60
		16.45	120.01	10.60		
		16.55	120.00	10.50		
6-18-48	3	16.84	120.14	10.28	10.35	10.70
		16.74	119.55	10.22		
		16.59	119.31	10.50		
		16.54	118.84	10.40		
6-21-48	3	17.29	123.84	10.35	10.41	10.76
		16.99	122.44	10.43		
		16.89	121.94	10.43		
		16.87	121.33	10.38		

APPROVED FOR PUBLIC RELEASE

- 78 -

APPENDIX III

Series #1

LA 710

Run No.	Δt Sec.	N_r Counts	N_p Counts	C Coincidences	$\dfrac{Cr}{N_p}$ Corr.
1	$1.800 \cdot 10^3$	$3.29 \cdot 10^4$	$1.737 \cdot 10^6$	75	$12.7 \pm 6.8 \cdot 10^{-6}$
2	1.800	2.80	1.536	59	12.5 ± 6.7
3	1.800	2.46	1.235	80	34.5 ± 9.0
4	1.800	2.165	.947	44	19.8 ± 9.0
5	1.800	2.940	1.727	94	18.2 ± 7.6
6	1.680	1.172	.747	33	28.8 ± 9.0
7	1.800	3.799	1.782	105	11.9 ± 8.2
8	1.805	3.269	1.517	88	17.8 ± 8.4
9	1.800	2.503	1.465	81	25.1 ± 7.9
10	1.800	2.055	1.180	66	30.7 ± 8.5
11	1.800	1.893	1.152	59	27.8 ± 8.2
12	2.355	1.650	1.000	45	29.6 ± 7.9
13	1.441	1.875	.997	44	15.2 ± 8.8
14	1.800	2.920	1.583	83	16.4 ± 7.9
15	1.800	1.341	.818	18	5.7 ± 7.0
16	1.744	1.428	.965	36	19.1 ± 7.7
17	1.620	1.534	.987	48	27.6 ± 8.6

- 79 -

APPENDIX III

Series #2

LA 710

Run No.	Δt Sec.	N_r Counts	N_p Counts	C Coincidences	$\dfrac{Cr}{N_p}$ Corr.
1	$1.800 \cdot 10^3$	$2.105 \cdot 10^4$	$.886 \cdot 10^6$	36	$19.0 \pm 8.6 \cdot 10^{-6}$
2	1.800	2.840	1.075	50	18.3 ± 8.7
3	1.800	2.580	.999	40	14.2 ± 8.4
4	1.800	2.450	.927	43	21.8 ± 8.9
5	1.800	3.050	1.107	45	7.05 ± 9.2
6	1.800	3.305	1.195	51	6.3 ± 9.4
7	1.800	3.230	1.120	41	5.0 ± 8.6
8	1.510	1.626	.522	17	13.8 ± 10.7

UNCLASSIFIED

APPENDIX IV

Series #3

LA 710

Run No.	Δt Sec.	N_f Counts	N_p Counts	C Coincidences	$\dfrac{Cr}{N_p}$ Corr.
1	$1.800 \cdot 10^3$	$3.235 \cdot 10^4$	$.752 \cdot 10^6$	41	$20.4 \pm 11.10 \cdot 10^{-6}$
2	1.800	3.180	.985	60	27.7 ± 10.15
3	1.800	2.981	1.020	66	33.5 ± 10.00
4	1.800	3.010	1.075	53	17.8 ± 9.02
5	1.800	3.300	.831	37	9.82 ± 10.05
6	1.800	3.001	.697	38	22.9 ± 11.40
7	1.764	2.685	1.025	54	24.2 ± 9.22
8	1.765	2.440	.882	37	15.83 ± 9.07
9	1.800	2.680	.721	37	23.20 ± 10.72
10	1.800	3.145	.977	37	4.75 ± 8.88
11	1.800	2.590	.990	39	13.50 ± 9.32
12	1.800	2.525	.967	39	13.40 ± 9.82
13	1.800	2.580	.955	38	15.20 ± 9.44
14	1.800	1.505	.419	15	20.2 ± 11.2
15	1.800	1.770	.512	17	14.55 ± 10.3
16	1.800	1.835	.550	18	13.52 ± 9.92
17	1.800	1.745	.470	18	20.05 ± 11.15
18	1.788	1.617	.442	19	26.10 ± 11.86
19	1.800	3.970	1.213	79	23.30 ± 10.24
20	1.800	3.520	1.184	60	14.08 ± 8.97

UNCLASSIFIED

DOCUMENT ROOM

REC. FROM Ed Dur

DATE 1-16-48

REC. NO. REC.